Deep Extragalactic Surveys around the Ecliptic Poles with AKARI (ASTRO-F)

Hideo Matsuhara,[1] * Takehiko Wada,[1] Shuji Matsuura,[1] Takao Nakagawa,[1] Mitsunobu Kawada,[2] Youichi Ohyama,[1] Chris P. Pearson,[1,11] Shinki Oyabu,[1] Toshinobu Takagi,[1,3] Stephen Serjeant,[3,12] Glenn J. White,[3,12] Hitoshi Hanami,[4] Hidenori Watarai,[5] Tsutomu T. Takeuchi,[6,13] Tadayuki Kodama,[7] Nobuo Arimoto,[7] Sadanori Okamura,[8] Hyung Mok Lee,[9] Soojong Pak,[10] Myung Shin Im,[9] Myung Gyoon Lee,[9] Woojung Kim,[1] Woong-Seob Jeong, [1] Koji Imai,[1] Naofumi Fujishiro,[1†] Mai Shirahata,[1] Toyoaki Suzuki,[1] Chiaki Ihara[1‡] and Itsuki Sakon[8]

[1] *Institute of Space and Astronautical Science, Japan Aerospace Exploration Agency, Sagamihara, Kanagawa 229 8510*

[2] *Graduate School of Science, Nagoya University, Chikusa-ku, Nagoya, 464-8602*

[3] *University of Kent, Canterbury, Kent CT2 7NR, UK*

[4] *Iwate University, 3-18-8 Ueda, Morioka, 020-8550*

[5] *ALOS Project, Japan Aerospace Exploration Agency, Tsukuba, Ibaraki 305-8505*

[6] *Laboratoire d'Astrophysique de Marseille, Traverse du Siphon, BP8 13376 Marseille Cedex 12, France*

[7] *National Astronomical Observatory of Japan, Mitaka, Tokyo 181-8588*

[8] *Department of Astronomy, School of Science, University of Tokyo, Bunkyo-ku, Tokyo 113-0033*

[9] *Astronomy Program, Seoul National University, Shillim-Dong, Kwanak-Gu, Seoul 151-742, Korea*

[10] *Kyung Hee University, 1 Seocheon-dong, Giheung-gu, Yongin-si Gyeonggi-do 446-701, Korea*

[11] *ISO Data Centre, ESA, Villafranca del Castillo, Madrid, Spain.*

[12] *Astrophysics Group, Department of Physics, The Open University, Milton Keynes, MK7 6AA, UK*

[13] *Astronomical Institute, Tohoku University, Aoba-ku, Sendai 980-8578*

(Received 2005 November 14; accepted 2006 April 28)

Abstract

AKARI (formerly ASTRO-F) is an infrared space telescope designed for an all-sky survey at 10-180 μm, and deep pointed surveys of selected areas at 2-180 μm. The deep pointed surveys with AKARI will significantly advance our understanding of galaxy evolution, the structure formation of the Universe, the nature of the buried AGNs, and the cosmic infrared background. Here we describe the important characteristics of the AKARI mission: the orbit, and the attitude control system, and investigate the optimum survey area based on the updated pre-flight sensitivities of

AKARI, taking into account the cirrus confusion noise as well as the surface density of bright stars. The North Ecliptic Pole (NEP) is concluded to be the best area for 2-26 μm deep surveys, while the low-cirrus noise regions around the South Ecliptic Pole (SEP) are worth considering for 50-180 μm pointed surveys to high sensitivities limited by the galaxy confusion noise. Current observational plans of these pointed surveys are described in detail. Comparing these surveys with the deep surveys with the Spitzer Space Telescope, the AKARI deep surveys are particularly unique in respect of their continuous wavelength coverage over the 2-26 μm range in broad-band deep imaging, and their slitless spectroscopy mode over the same wavelength range.

Key words: space vehicles: instruments — galaxies : evolution — galaxies : statistics — infrared galaxies

1. Introduction

How did the galaxies form and evolve? How did the clusters of galaxies and the large-scale structure of the Universe form and evolve? How do the Active Galactic Nuclei (AGN) link together with the Ultralumonius Infrared Galaxies (ULIRGs) in their birth and evolution? What is the nature of the sources contributing to the Cosmic Infrared Background (CIRB)? In order to answer these important questions of modern astronomy we need statistically significant numbers of sources based on large-area surveys to uniform depths covering significant cosmological volumes. Such surveys should be made in many wavebands, since multi-wavelength spectral energy distributions (SEDs) as well as photometric redshifts are useful to identify the types and ages of the detected galaxies.

Naturally, there is a trade-off, between the area and the depth of any survey, with a greater required depth resulting in a narrower survey due to the finite observation time. For example, at wavelengths shorter than 2 μm, towards two blank fields, the Hubble Space Telescope (HST) has produced excellent images to unprecedented sensitivity and angular resolution (Hubble Deep Fields: HDF), but they were limited to relatively small areas (HDF-N, 5.3 arcmin^2, Williams et al. 1996 and HDF-S, 0.7 arcmin^2, Gardner et al. 2000; Williams et al. 2000). Recently, thanks to the *Advanced Camera for Surveys* onboard the HST, very large deep survey programs such as the Great Observatories Origins Deep Survey (GOODS, 320 arcmin^2, Giavalisco et al. 2004) and the Galaxy Evolution from Morphology and SEDs survey (GEMS, 795 arcmin^2, Rix et al. 2004), have also been performed. A 1.5 deg^2 survey

* Further information contact Hideo Matsuhara (maruma@ir.isas.jaxa.jp)

† Present address : Genesia Corporation, Mitaka, Tokyo 181-0013

‡ Present address : NEC Aerospace systems, Ltd., Fuchu, Tokyo 183-8501

program is now on-going (COSMOS project[1]).

Longer infrared wavelengths beyond 2 μm are undoubtedly very important. The stellar mass of a galaxy is a fundamental property of galaxies, and is well traced by the near-infrared ($1-2\,\mu$m) light. Since ground-based telescopes are not sensitive enough to detect the stellar light beyond $2\,\mu$m, space-borne telescopes are essential for the study of the galaxy stellar mass at high redshift. Mid-IR wavelengths are also important because they are sensitive to dusty star forming galaxies which are characterized by the PAH features as well as the hot dust continuum. This fact had previously been recognized by the first all-sky survey in the mid- and far-infrared with the *Infrared Astronomical Satellite* (IRAS, Neugebauer et al. 1984). After the launch of the *Infrared Space Observatory* (ISO, Kessler et al. 1996), which executed many infrared surveys covering a wide range in both depth and area at 7, 15, 90, and 170 μm, various mid- to far-infrared SEDs of starburst galaxies as well as AGN (Genzel, Cesarsky 2000 and references therein) have been revealed and investigated to great detail. The ISO surveys and their follow-up spectroscopic observations have demonstrated the importance of the mid- to far-infrared wavelengths in the study of evolution of galaxies (HDF-S: Franceschini et al. 2003, FIRBACK Marano: Patris et al. 2003, ELAIS-S1/S2: Pozzi et al. 2004, Lockman Hole: Oyabu et al. 2005).

In August 2003, NASA launched an advanced space infrared observatory, the *Spitzer Space Telescope* (*Spitzer*; formerly SIRTF, Werner et al. 2004). offering the capability of deep imaging from 3-160 μm and spectroscopy from 5-38 μm. In February 2006, JAXA (Japan Aerospace eXploration Agency) launched a complementary infrared astronomy satellite AKARI (formerly known as ASTRO-F[2]). AKARI will observe at near- to far-infrared wavelengths like *Spitzer*. It should be emphasized that AKARI is primarily a surveyor mission, though it has an additional role as an observatory with unique capabilities complementary to *Spitzer*. A detailed comparison of these two missions are given in section 6.2. It is expected that AKARI will also provide an invaluable database for the planning of observations with the *Herschel* Space Observatory (Pilbratt 2003).

In this paper, we describe the planned three major extragalactic deep surveys with AKARI:

- a deep 2-26 μm survey at the North Ecliptic Pole (NEP), covering a 0.5 deg^2 area, to a 5σ flux limit of 10-30 μJy at 11-18 μm,
- a wide, shallow 2-26 μm survey at the NEP, over a 6.2 deg^2 area, to a 5σ flux limit of 60-130 μJy at 11-18 μm. The survey region is a circular area surrounding the " NEP-Deep" field, and in total 450 pointing observations are required.
- a deep 50-180 μm survey towards a low-cirrus region near the South Ecliptic Pole (SEP)

[1] See http://www.astro.caltech.edu/ cosmos/

[2] ASTRO-F was successfully launched on 21st February, 2006, and has been re-named *AKARI*.

Table 1. Overview of the planned AKARI extragalactic deep surveys

Name	Field Center (J2000)	Field Size and Shape	Imaging Bands and Depth
NEP-Deep	$17^{\rm h}55^{\rm m}24\overset{\rm s}{.}00$ $+66°37'32\overset{''}{.}0$	0.5 deg^2 circular	all IRC, FIS (Table 6)
NEP-Wide	$18^{\rm h}00^{\rm m}00\overset{\rm s}{.}00$ $+66°36'00\overset{''}{.}0$	6.2 deg^2 circular	all IRC, FIS (Table 6)
SEP Low-Cirrus	$4^{\rm h}44^{\rm m}00\overset{\rm s}{.}00$ $-53°20'00\overset{''}{.}0$	15 deg^2 fan-shape	S9W, S18W, all FIS (Table 3)

: covering 15 deg^2, down to the confusion limit due to unresolved galaxies.

The location of fields are summarized in Table 1. In section 2 we present the AKARI mission, and detail its observing modes. We then describe the key science objectives of the AKARI deep surveys in section 3. In section 4 we discuss the various constraints on the survey characteristics, such as the visibility, confusion due to infrared cirrus and saturation from bright stars. Section 5 details the observing plan. Section 6 compares these surveys with other infrared surveys with ISO and *Spitzer*. In section 7 we review the current status of our ground based preemptive observations. The summary is given in section 8. Throughout this paper we assume a flat concordance cosmology of $\Omega_{\rm M} = 0.3$, $\Omega_\Lambda = 0.7$ and $H_0 = 72\,{\rm km\,s^{-1}\,Mpc^{-1}}$.

2. The AKARI Mission Outline

AKARI will be a second generation infrared sky survey mission after IRAS with much improved sensitivity, spatial resolution and wider wavelength coverage. During the expected mission life of more than 500 days, AKARI will make an all-sky survey in 6 wavebands in the mid- to far-infrared since IRAS, and the first ever all-sky survey at 100-160 μm. In addition to the all-sky survey, deep imaging and spectroscopic observations in the pointing mode will also be carried out in many wavebands covering 2-160 μm. The observation strategy in this mode was discussed in Pearson et al. (2001) based on the preliminary mission specifications. This paper describes the deep extragalactic surveys, based on the updated pre-flight specifications of the mission. The expected results of the deep pointed surveys will appear in an updated version of the above paper based on the in-flight sensitivities (Pearson et al. 2006, in preparation).

AKARI is equipped with a 68.5-cm cooled (approximately to 6K) Ritchey-Chrétien type telescope and two focal plane instruments covering the 2-180 μm wavelength range. Details of the AKARI mission and satellite system are described in Murakami (2004), and details on the current performance of the focal plane instruments are described in Kawada et al. (2004) and Onaka et al. (2004).

2.1. AKARI orbit and observation modes

The orbit of AKARI is a sun-synchronous polar orbit at an altitude of 750km and an inclination of 98.4 deg. The orbital period is approximately 100 minutes. In Figure 1, the

Table 2. Parameters of the AKARI Orbit and Operations

Orbit Parameters	
Altitude	750 km
Period	99.83 minutes
Mean motion of Argument of Perigee	0.9856 deg day^{-1}
Operational Parameters	
Maximum offset angle out of the observing plane	$\pm$1 deg
Roll angle offset	not used
Maneuver time from the survey mode to the pointing mode	450 sec
Attitude stabilization time before the pointed observation	300 sec max.
Duration of a pointed observation	600 sec nominal
Maneuver time from the pointing mode to the survey mode	450 sec

AKARI spacecraft attitude is shown schematically. In the all-sky survey mode, the spacecraft rotates uniformly around the axis directed toward the Sun once every orbital revolution, resulting in a continuous scan of the sky on one orbit. In this configuration, the entire sky can be covered in half a year. In the attitude operation for pointed observations (Figure 1 right), due to the limitations imposed to prevent earthshine from illuminating the telescope baffle, the duration of any single pointed observation is limited to 10 minutes. The pointing direction can be freely chosen in the telescope orbital plane given by the survey mode attitude. However, it is restricted to within $\pm$1 deg to the direction perpendicular to the orbital plane[3]. The attitude control system provides an additional capability to slightly change the pointing direction defining the following attitude modes: step-scan, slow-scan, and micro-scan. The slow-scan is a uniform scan with much slower scan speed (less than 30 arcseconds per second) than that of the all-sky survey, and is an option for pointed observations with AKARI. Hence the duration of this observing mode is also limited to 10 minutes. The slow-scan survey is especially useful for covering a larger sky area than that obtainable by pointing toward the fixed direction in the sky to much better sensitivities than those of the all-sky survey. One should note that the overheads in the pointing attitude mode are significant: approximately 20 minutes is required for the maneuvering and stabilization. Hence the number of pointing observations in one orbit is restricted to three or less (see Table 2).

2.2. Scientific instruments

AKARI incorporates two focal plane instruments covering the infrared wavelength range from 2 to 160 μm. The first focal plane instrument is the Far-Infrared Surveyor (FIS, Kawada

[3] We hereafter call this function of the attitude control system "offset control" which allows the telescope to be directed out of the nominal orbital plane up to $\pm$1 deg.

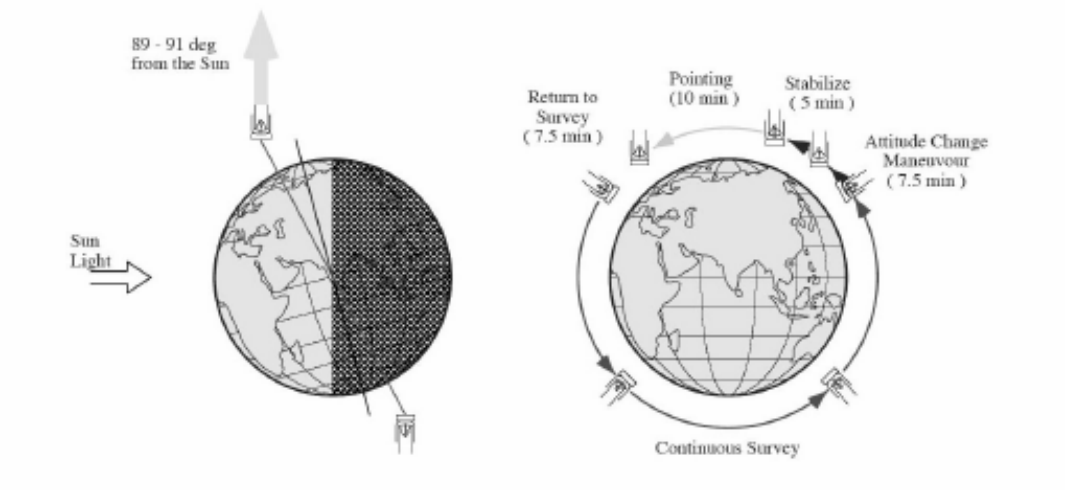

Fig. 1. The AKARI spacecraft attitude is shown schematically. (Left) the all-sky survey mode. (Right) the attitude operation for the pointed observations. The duration of a single pointed observation is limited to approximately 10 minutes. The pointing direction is restricted to within ±1 deg in the direction perpendicular to the orbital plane.

et al. 2004) which will primarily survey the entire sky simultaneously in four far-infrared bands from 50 to 160 μm with approximately diffraction-limited spatial resolutions (30-60 arcsec, Jeong et al. 2003). Each waveband is equipped with corresponding far-infrared imaging arrays denoted as: N60, WIDE-S, WIDE-L, and N160, all of which are operated simultaneously. The second focal-plane instrument is the InfraRed Camera (IRC, Onaka et al. 2004), which is primarily designed to take deep images of selected regions of sky by pointed observations from 2 to 26 μm. The IRC comprises of three channels: NIR(2-5 μm), MIR-S(5-12 μm), MIR-L(12-26 μm). These three channels can be operated simultaneously. The waveband characteristics for broad-band imaging are summarized in Table 3 and Figure 2 Each IRC channel is equipped with 3 broad-band imaging bands, which have to be selected by rotating a filter wheel. Both focal plane instruments are equipped with spectroscopic elements of moderate or low resolution : the FIS is equipped with a Fourier-Transform Spectrometer (FTS) covering 50-180 μm using the WIDE-S and WIDE-L detector arrays, while the IRC is equipped with low-dispersion grisms (and a prism in the NIR channel) which enable slitless spectroscopy over the field-of-view (FOV) of each channel with spectral resolutions of 40-90 at 2-26 μm. The IRC also has the capability for slit spectroscopy.

Figure 3 shows the FOV configuration projected onto the sky. Note that the NIR and the MIR-S channels observe the same sky simultaneously, while the FOV of the MIR-L channel is offset by approximately 25 arcmin from the NIR and the MIR-S channels. During the pointing observations, all focal plane instruments are operated simultaneously although the target is acquired through a selected FOV of either the NIR/MIR-S, MIR-L, or FIS. Hence parallel-

Table 3. Specifications of IRC and FIS filter bands and the flux limits in various observing modes

Band (IRC)	λ_c (μm)	$\Delta\lambda$ (μm)	All-sky survey (5σ, mJy)	Slow-Scan(15"sec^{-1}) (5σ, mJy)	Pointing* (5σ, μJy)
N2	2.43	0.68	N/A	N/A	7.9
N3	3.16	1.12	N/A	N/A	3.7
N4	4.14	1.22	N/A	N/A	7.2
S7	7.3	2.6	N/A	11	33
S9W	9.1	4.3	80	7	26
S11	10.7	4.7	N/A	13	37
L15	15.7	6.2	N/A	16	68
L18W	18.3	10.0	130	20	87
L24	23.0	5.4	N/A	53	180
Band (FIS)	λ_c (μm)	$\Delta\lambda$ (μm)	All-sky survey† (5σ, mJy)	Slow-Scan(15"sec^{-1})† (5σ, mJy)	Pointing (5σ, μJy)
N60	65	21.7	1000	70	N/A
WIDE-S	90	37.9	200	14	N/A
WIDE-L	140	52.4	400	9	N/A
N160	160	34.1	800	18	N/A

* in case of the astronomical observation template (AOT) for deep imaging with no filter change and no dithers at Ecliptic poles. Net exposure times in this AOT are 459 sec per pointing for the NIR, and 513 sec per pointing for the MIR-S/MIR-L channels, respectively. Photometric apertures are determined so that the signal-to-noise ratio for the source is maximized with the expected point-spread function at each waveband (typical aperture radius is 1-2 pixels).

† sensitivity for one scan. Surveys with at least two scans (all-sky survey) or four scans (SEP low-cirrus region survey) are planned.

mode observation, *i.e.* observation with channels which do not observe the same field of view in the sky, is always executed as long as this does not have any impact on the data rate or does not induce heat dissipation to the AKARI cryostat, which would shorten the mission life. The pre-flight sensitivities estimated from the current laboratory experiments of the telescope and the focal plane instruments at low temperatures are shown in Tables 3 and 4. The IRC sensitivity is given for its single-filter astronomical observation template (AOT), in which no filter change is made during a single pointed observation, such that each IRC channel observes the target with a single filter. There are also two-filter or three-filter AOTs as well as an AOT dedicated for the spectroscopy. The FIS broad-band sensitivity in pointing mode is not available since only the FTS will be used in the pointing observation mode. The FIS sensitivity in the slow-scan attitude mode is shown, since the slow-scan survey is useful to observe larger areas within the limited time of a single pointed observation.

Table 4. Specifications of IRC spectroscopic channels

Band	Wavelength Coverage (μm)	Spectral Resolution ($\lambda/d\lambda$) †	Flux limit (continuum) * (per pixel, 5σ, mJy)
NP	1.7 – 5.5	22	0.02
SG1	5.5 – 8.3	47	1.0
SG2	7.4 – 13.	34	3.2
LG2	17.7 – 25.	27	6.7

* in case of one pointing observation at ecliptic poles with the AOT for the "slitless spectroscopic mode", where the source spectra are dispersed in the imaging area of the detector array.

† λ is the center wavelength, and $d\lambda$ is a wavelength resolution corresponding to the FWHM size of the point spread function.

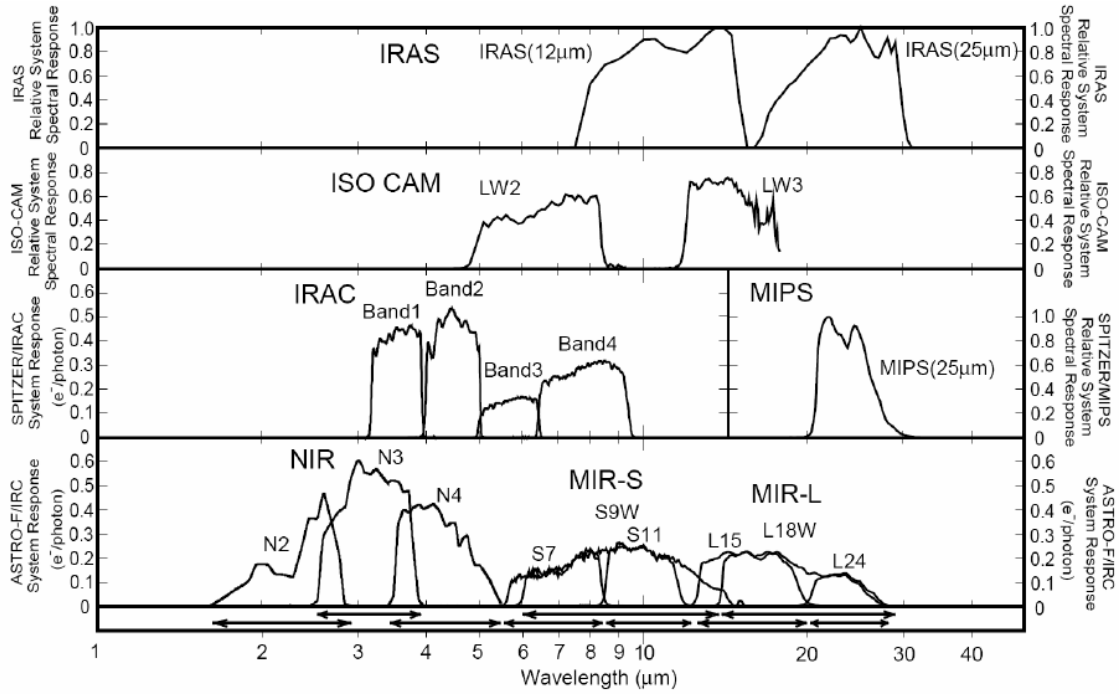

Fig. 2. Comparison of spectral responce curves of AKARI wavebands for imaging and survey with those of other infrared astronomical satellites. Those of ISO and IRAS are relative, while those of *Spitzer* and AKARI are absolute in units of electrons per photon.

2.3. Mission phases and observation programs

Observations with AKARI can be divided into the following phases:

- PV phase [L(launch)+1 – L+2months] : observations for performance verification of the whole system.

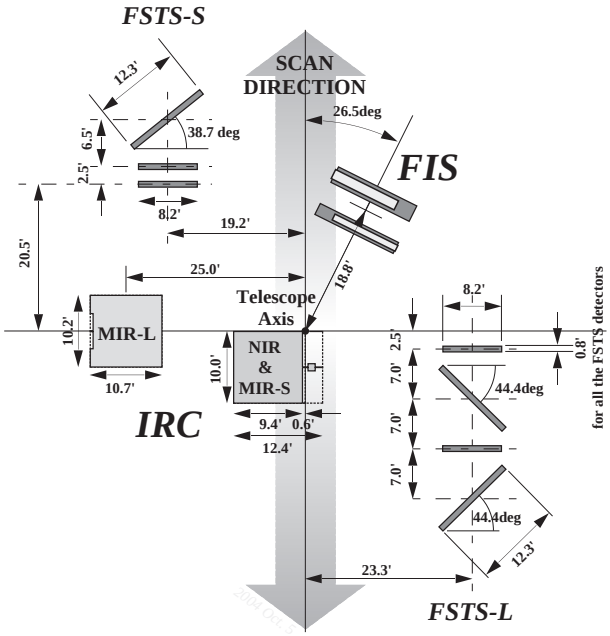

Fig. 3. Configuration of the field-of-views of the AKARI focal-plane instruments, projected onto the sky.

- Phase 1 [L+2 – L+8months] : primarily for the all-sky survey. However, pointed observations toward fields close to the ecliptic poles are planned for orbits passing through the South Altantic Anormaly (SAA).
- Phase 2 [L+8 – L+18months (boil-off of liquid He)] : supplemental all-sky survey observations for areas not sufficiently covered in phase-1, and pointed observations in any region on the sky.
- Phase 3 [after boil-off of liquid He] : pointed observations with the IRC-NIR channel which will continue to function even after the boiling-off of the liquid He. The duration of this phase is uncertain and is limited by the life of the mechanical coolers.

During the AKARI mission phases above, the following observation programs are planned:

- Large-area Survey (LS): the all-sky survey, the primary objective of the AKARI mission, as well as large-area *Legacy* surveys in pointing mode over two dedicated fields near the ecliptic poles: the NEP (section 5.2) and the Large Magellanic Could (LMC). The outline of the LS programs are described in Matsuhara et al. (2005).
- Mission Programs (MP): an organized program of pointed observations planned by the AKARI science working groups (AKARI team plus collaborators within the international astronomical community). The targets are spread over large areas but cannot be included in the NEP and LMC surveys.
- Open-time Program (OP): a program of pointed observations open to the Japanese, Korean, and ESA communities. 30% of the total pointed observation opportunities in

both phases 2 and 3 will be allocated to OP.

- Director's Time: observing time allocated to the Project Manager, including any "Target of Opportunity" time. Less than 5% of the total observation is considered so far.
- Calibration Time: for the long-term maintenance and performance verification for each instrument, calibration observations will be made at regular periods.

3. Key Scientific Objectives

Here we describe the key scientific objectives of the AKARI deep pointed observation extragalactic surveys, and also discuss the optimal survey area and depth.

3.1. Mass assembly and structure evolution

The total stellar mass of a galaxy is well traced by the near-infrared luminosity at 1-2 μm where the effects of star-formation are small compared to optical wavelengths. The evolution of the stellar mass function of the galaxy provides a basic piece of information for modern cosmology. Moreover, the galaxy's stellar mass can be used as a tool to reveal the evolution of the large-scale structure of the Universe, if a sufficient number of galaxies are sampled over a large enough cosmic volume. Since the spectroscopic determination of the redshift of galaxies in such a large sample is extremely time and effort consuming, the "photo-z" technique, a method of the determination of redshift based on multi-wavelength data, has been widely used (see *Hyper-z*: Bolzonella et al. 2000, Baysian method: Benítez 2000, *ANN-z*: Collister, Lahav 2004), Dickinson et al. 2003 (HDF-N), Fontana et al. 2004 (K20 survey) for examples). Since ground-based telescopes are not sensitive enough to detect the stellar light beyond 2 μm, the photo-z technique has been thus far based on the 0.4 μm break and the Lyman break. On the other hand, space-borne telescopes, such as *Spitzer* and AKARI, can observe longward of 2 μm and can thus execute a systematic study of the galaxy stellar mass at high redshifts. Furthermore, there is another redshift estimator in the rest-frame 1.6 μm where the H^- opacity minimum of the stellar atmosphere (Sawicki 2002) exists. The 4 *Spitzer*/IRAC wavebands are specially designed to determine the photometric redshift by using this bump. The near-infrared and shorter mid-infrared filter bands of IRC (see Table 3) continuously cover the $2-10\,\mu$m wavelength range and hence a systematic study of the galaxy mass at various redshifts is also possible. Figure 4 shows the tracks of typical normal galaxies for z=0-4 on a two colour diagram for the IRC wavebands. For the determination of the mass function in each redshift bin, a mass sensitivity to well below 10^{11} $M_\odot$ (*i.e.* charanteristic stellar mass M_* of the Schechter function, see Dickinson et al. 2003) is required. As shown in Figure 5, 10 pointing observations in the N3 and N4 bands satisfy this requirement out to z=4. In this plot $z_{form} = 20$ is assumed to demonstrate the high sensitivity to the stellar mass even at high redshifts.

Here we discuss the requirement for the survey volume. We require statistically sig-

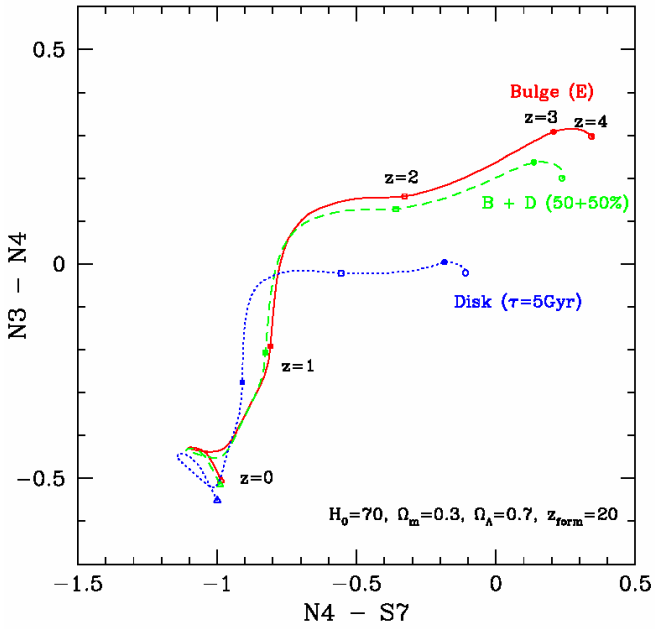

Fig. 4. Tracks of early and late type galaxies on the two colour ([N4] - [S7] vs [N3] - [N4] in AB magnitudes) diagram. The SEDs are calculated from the model of Kodama, Arimoto (1997).

nificant numbers of galaxies detectable with AKARI at each redshift bin. If the source of uncertainty is solely Poisson error, one could simply request ≥ 100 sources per redshift bin with 10% accuracy. However, for relatively small survey volumes, observational estimates of the number density of the galaxies suffer from the cosmic variance - the field-to-field variation due to the large scale structure. For example, in case of a 0.5 deg^2 area, the comoving volume for Δz=0.2 intervals at z=2-3 is 1.1×10^6 Mpc^3, corresponding to a cube of side length of 100Mpc. According to Somerville et al. (2004), the uncertainty due to the cosmic variance for strongly clustered populations such as EROs is estimated to be 30-40%, while for less clustered populations it is around 15-20%(for LBGs). The cosmic variance shows a rather weak dependence on the survey volume V: $V^{\gamma/6}$ where γ is the index of the two-point correlation function, and therefore a factor of two reduction of the variance requires an order of magnitude larger volume which cannot be easily obtained by the on-going space infrared telescopes. It should be noted however, that Peacock, Dodds (1994) described the power spectra obtained by optical large-area surveys as well as the IRAS survey which gives only 3-4% cosmic variances for 0.5 deg^2 area with Δz=0.2 interval. In conclusion at $z \geq 1$ a 0.5 deg^2 area is our minimum requirement to avoid serious effects due to cosmic variance, while for $z \leq 1$, more than 5 deg^2 area is recommended.

The survey area and depth requirements to obtain the desired scientific objectives de-

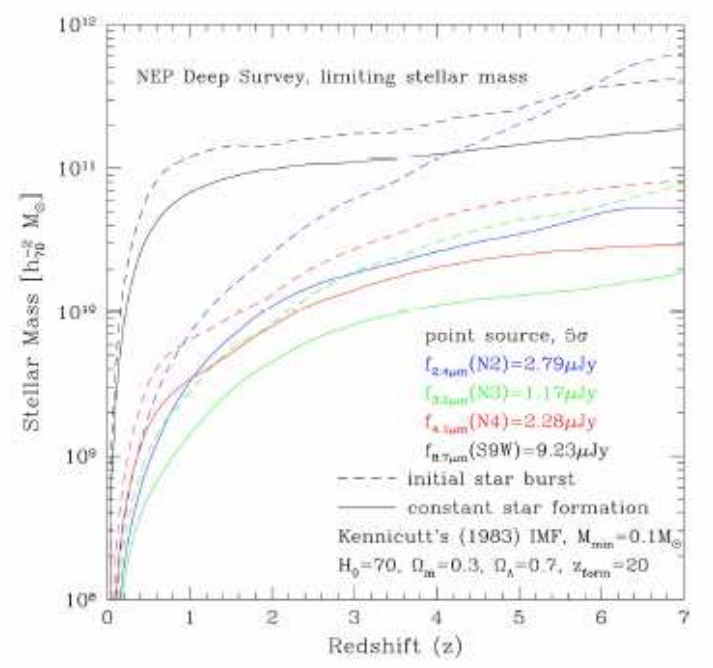

Fig. 5. Minimum detectable stellar mass of galaxies as a function of redshift for 8(N2), 10(N3, N4) pointing observations per filter with AKARI/IRC. Two extreme cases of the star-formation history are assumed: an initial burst (dashed lines) and constant star-formation (solid lines) to form the stellar mass at the detection limit during the age of the galaxy .

scribed in this subsection are summarized as follows:

- survey depth: sensitivity for the stellar mass of a galaxy: $< 10^{11}$ M$_\odot$ out to z=4. Approximately 10 pointing observations are required for the 2-9 μm wavebands.
- survea area : 0.1 deg^2 is not suffcient to overcome the cosmic varience, however, 0.5-1 deg^2 area is reasonable at $z = 1-4$ if a 10-30% cosmic variance effect is acceptable.

3.2. Dusty star-formation history of the universe

In the past few years considerable progress has been made in the understanding of the star formation rate of high-z galaxies using the Lyman drop out technique to identify galaxies at $z = 3-5$ (Steidel et al. 1996; Ouchi et al. 2004). Well over 2000 Lyman-break systems have now been observed at $z > 3$. These are ultraviolet (UV)-bright, actively star-forming galaxies with blue spectra and star formation rates of a few to $\sim 50\,\mathrm{M_\odot yr^{-1}}$. Moreover, thanks to the commissioning of very deep large-area surveys with narrow-band filters on 8-m class telescopes, more than twenty Lyα-emitting(LAE) galaxies at $z > 5$ have been identified (Taniguchi 2003, Shimasaku et al. 2004, Ouchi et al. 2005), providing us with the first insight into the star formation history of the Universe beyond z=5. Typical star formation rates (SFR) of $z = 5-6$ LAEs are $5-10\,\mathrm{M_\odot yr^{-1}}$, which however should be considered as a lower limit, since a blue half

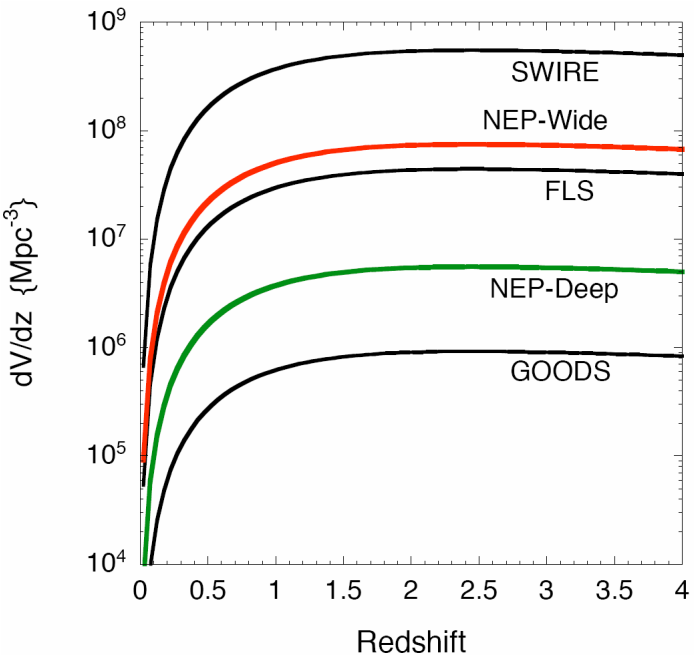

Fig. 6. Comparison of the comoving volume per unit redshift for *Spitzer*/GOODS, SWIRE and proposed AKARI deep surveys("NEP-Deep" and "NEP-Wide").

of the Lyα emission may be absorbed by HI gas and dust grains within the galaxy itself, and by the intergalactic HI gas.

The popular Madau plot (Madau et al. 1996) implied that the SFR of the Universe peaked at $z = 1-2$, although the SFR derived from the rest-frame optical/UV light has serious uncertainties in the correction of the dust extinction. However, the stellar mass of a galaxy derived from SED fitting including the K-band does not suffer so critically from the extinction corection, and it has been revealed that stellar mass density of the Universe as a function of redshift shows a rapid increase in the stellar mass density at $z = 1-2$, based on deep and wide $K_{\rm s}$ band surveys (Caputi et al. 2004, 2005). Furthermore, galaxies selected from optical and near infrared photometry with $BzK = (z'-K)_{\rm AB} - (B-z')_{\rm AB} > -0.2$ have been found to show active star formation rates of $> 100\,{\rm M}_{\odot}{\rm yr}^{-1}$ at $z > 1.4$ (Daddi et al. 2004). Therefore, it is very important to understand the star formation history of the Universe not only at $z > 4$ but also at $z = 1-2$.

It has been revealed that a significant portion of the energy emitted in the early Universe came not only from UV-selected galaxies but also from very luminous galaxies in the far infrared (FIR), that are hidden at optical wavelengths because of obscuration from interstellar dust grains. Recent submillimeter deep surveys with the SCUBA instrument on the JCMT have shown the existence of numerous such sources, showing that the sub-mm galaxies represent an important component of the cosmic star formation at high redshifts. For example, from

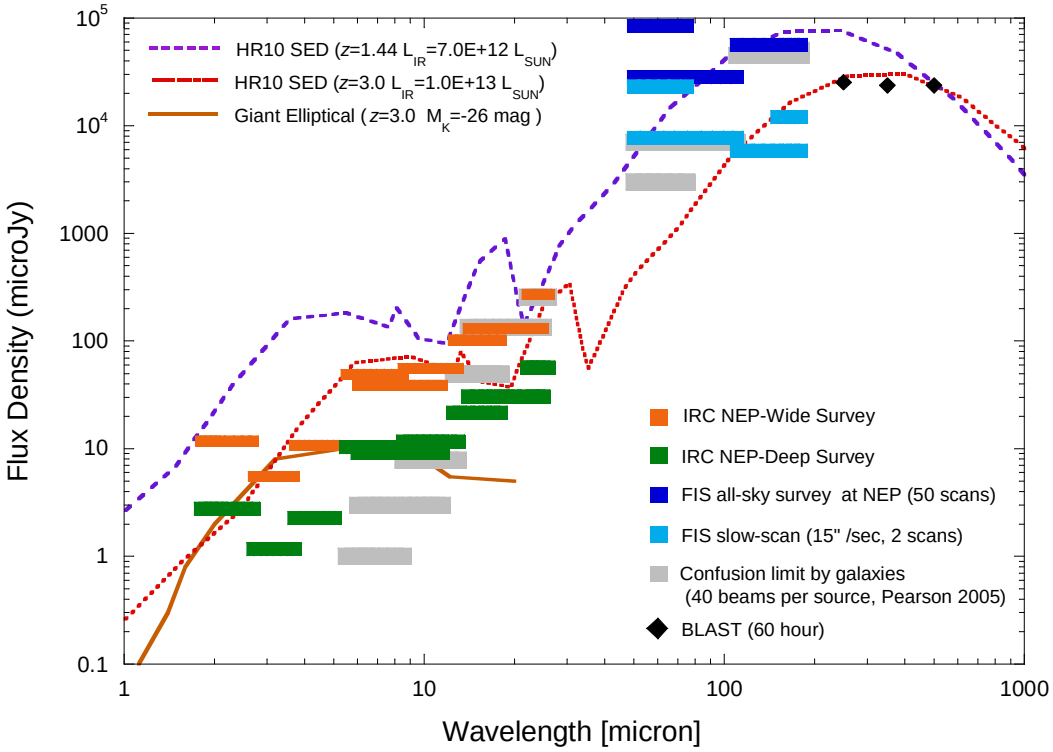

Fig. 7. 5σ sensitivities in micro Jansky for the IRC instrument in pointing mode ("Deep" and "Wide" surveys, see section 5) and the FIS instrument in the all-sky survey mode as well as in the slow-scan mode. Also shown for reference are the assumed spectral energy distributions of a normal spiral galaxy at z=3 (rest-frame absolute K = −26 mag (in Vega)) and dusty ERO spectral energy distributions at redshifts of 1.44 and 3 modeled on the archetypical ERO HR10. The source confusion due to galaxies have been included from the recently updated evolutionary models of Pearson (2005).

the follow-up optical spectroscopy with multi-object spectrographs on 10-m class telescopes. Chapman et al. (2003, 2005) have reported a median redshift of 2.3 for their sample of sub-mm galaxies with VLA identifications.

Since the submillimeter galaxies are very faint at optical wavelengths (UV in their rest frame) due to extinction by dust in the systems themselves, mid- and far-infrared observations with space infrared telescopes such as *Spitzer* and AKARI are critical to unveil their true nature. Such infrared observations will give unique information on their infrared SEDs which is an important clue to obtain information on the mass-to-light ratio, the overall dust opacity, and to infer the hidden star formation rate of these galaxies.

From these consideration, we propose to concentrate on the dusty star formation history at z=1-3 with AKARI, and generate statistically meaningful numbers of samples (order of 100-1000) in each redshift bin. Figure 7 shows the expected flux limits for the AKARI wavebands as well as the SED of a hyper-luminous ($L_{\rm IR} = 10^{13}\,L_{\odot}$) ERO at z=3. Quantitative discussion on the expected number of sources in the far infrared was given in Jeong et al. (2004), and

its revision including the near and mid infrared source counts can be found in Pearson et al. (2006) (in preparation). Figures 8, 9 show predicted fluxes of ULIRGs as a function of redshift for the IRC and FIS wavebands used for the proposed survey toward the ecliptic poles. Fluxes for various ULIRG SEDs with infrared luminosity of $3 \times 10^{12}\,L_{\odot}$ (Takagi, Pearson 2005) are shown. Note that if there are AGN contributions, the ULIRGs should be brighter than that expected from this model. Hence in order to detect ULIRGs at z=2-3 in the mid infrared, 8-10 pointing per filter, *i.e.* the depth proposed for the "NEP-Deep" survey, is sufficient. It should also be noted that the FIS slow-scan survey can potentially detect the far-infrared emission of the $z \sim 2$ mid-infrared sources in the "NEP-Deep" field (Figure 9).

Figure 6 shows a comparison of the comoving volume per unit redshift interval for *Spitzer*/GOODS (160 arcmin^2 for CDF-S, Giavalisco et al. 2004, *Spitzer*/SWIRE(50 deg^2, Lonsdale et al. 2004), and for the proposed AKARI NEP surveys. As discussed in section 3.1, a 0.5 deg^2 survey provides the sufficient cosmic volume for $z \geq 1$.

The survey area and depth requirements to obtain the desired scientific objectives described in this subsection are summarized as follows:

- survey depth: the sensitivity to detect ULIRGs at high redshift, for example, ($L_{\rm IR} = 10^{13}\,L_{\odot} < 10^{11}$ M$_{\odot}$ out to z=3. In particular, the 11-24 μm wavebands are important, and approximately 10 pointing observations are required in each band.
- survea area : 0.1 deg^2 is not suffcient to overcome the cosmic variance, however, a 0.5-1 deg^2 area is reasonable for $z = 1 - 3$ if 10-30% cosmic varience can be acceptable. Below $z < 1$ a 5-10 deg^2 area is preferable.

3.3. Unveiling the nature of the cosmic infrared background

Our knowledge of the Cosmic InfraRed Background (CIRB) at both near and far infrared wavelengths have been drastically increased by observations with COBE (Hauser, Dwek 2001, Lagache et al. 1999, Wright et al. 2004) and the Japanese IRTS mission (Matsumoto et al. 2005). In the near infrared, the observed 2 μm brightness of CIRB is more than a factor of two larger than that estimated by ultra-deep galaxy counts based on large ground-based telescopes (Totani et al. 2001, Matsumoto et al.), suggesting the existence of a contribution from a new population, such as the first stars (Kashlinsky (2005) and references therein). From the IRTS results Matsumoto et al. found a signiture of a break at 1-2 μm in the SED of the CIRB, and the existence of a bump in the power spectrum of the spatial fluctuation of the CIRB. The IRC onboard AKARI has spectroscopic capability in the near infrared to $\geq 2\,\mu$m. Moreover for this study, the IRC is very powerful because of its higher spatial resolution than those of COBE and IRTS as well as the high point-source sensitivity which will enable us to subtract any foreground point-like sources (stars and galaxies). Hence we will be able to investigate the small scale spatial fluctuations of the residual background. With IRTS, an appreciable spatial correlation at the 1-2 degree scale has been reported, therefore at least a survey scale of 2-4 degrees is

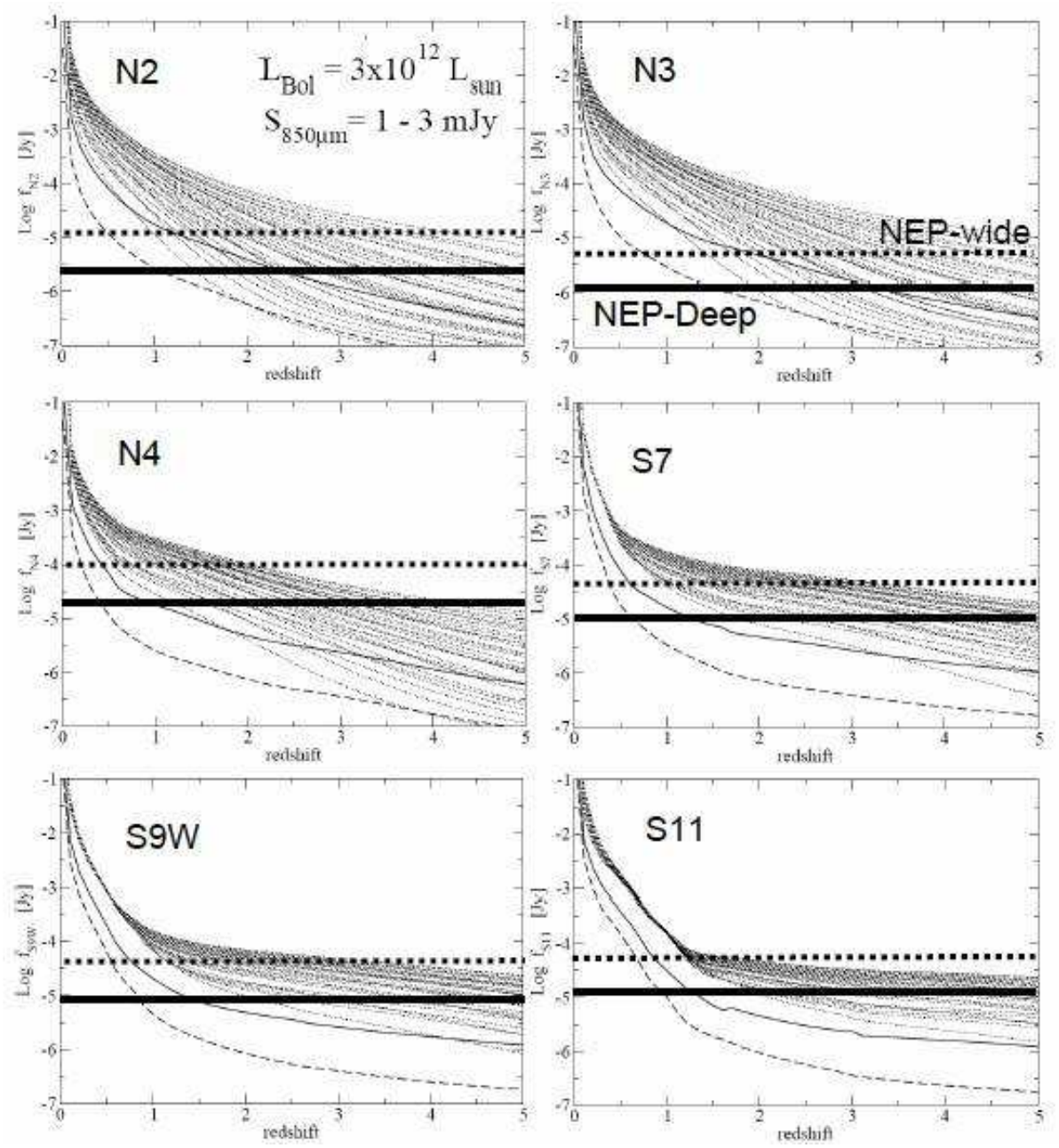

Fig. 8. Predicted fluxes of ULIRGs as a function of redshift for the IRC-NIR and IRC-MIR-S bands. The SED variation is determined from the observed SED of submm galaxies at $z = 2-3$ (Takagi, Pearson 2005). The luminosity is assumed to be $3 \times 10^{12} L_{\odot}$. Thick solid and dashed lines indicate the expected fluxes from Arp 220 and M82. The horizontal lines indicate the flux limits of the NEP survey with the IRC (dashed : for "NEP-Wide", solid : for "NEP-Deep").

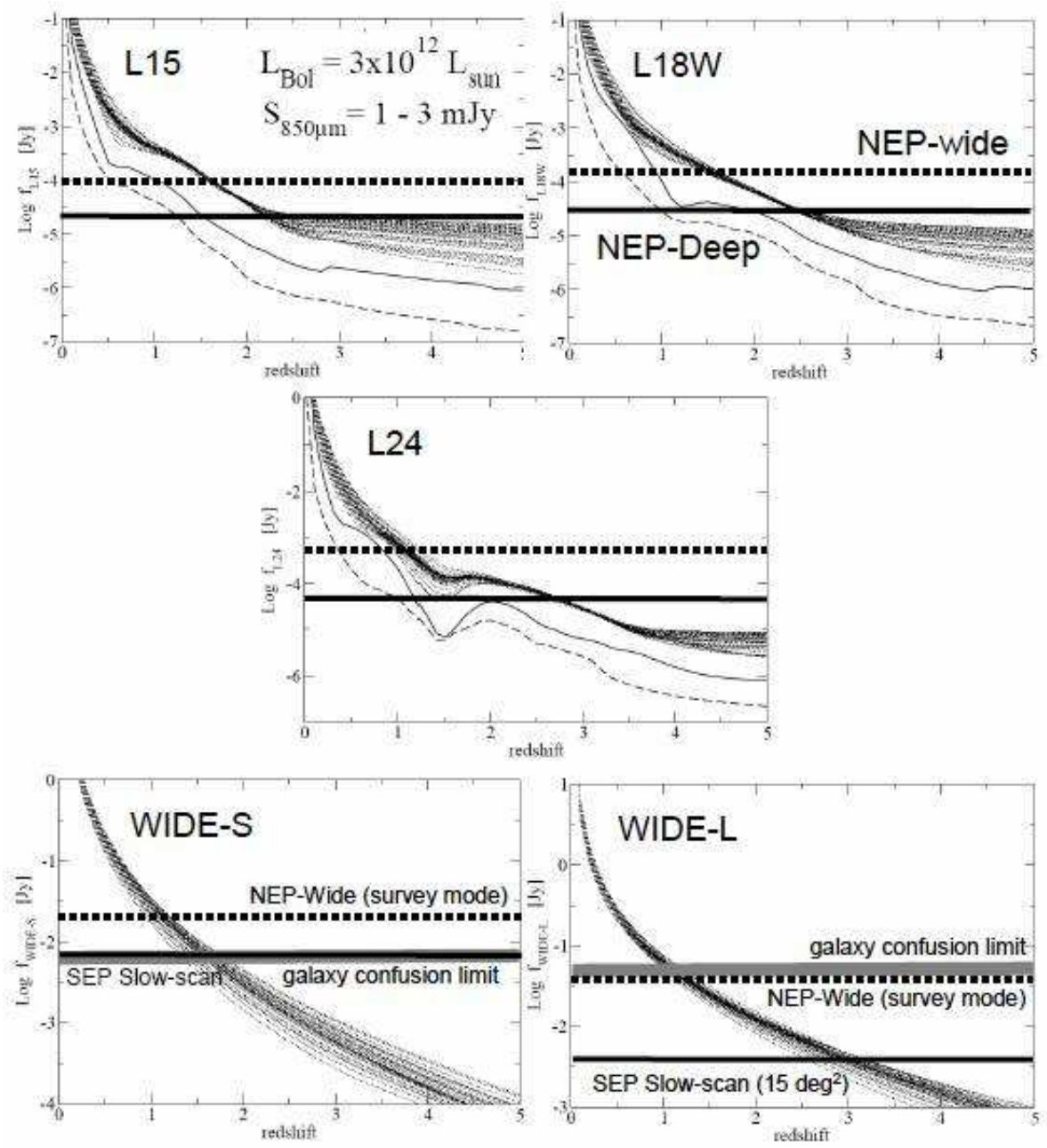

Fig. 9. Same as Figure 8, but for the IRC-MIR-L and the FIS bands.

required to obtain good statistical samples of such correlation signals. Supplemental data at various ecliptic latitudes are also necessary to subtract the contribution of the zodiacal light.

In the far infrared, not only the brightness of the CIRB but also its spatial fluctuations have been studied by observations with ISO (Lagache, Puget 2000, Matsuhara et al. 2000). However the source confusion limit is more serious than in the near-to-mid infrared due to the larger diffraction-limited beam size, inhibiting the detection of high redshift sources. On the other hand, the fluctuation power of the surface brightness of the sky, after excluding the bright point sources, contains information on the sources located at relatively high redshift. Hence, the fluctuation study is a very powerful tool to understand the nature of the sources responsible for the CIRB. Figure 10 shows the angular power spectra of the surface brightness fluctuations in the far infrared, observed with *ISO* and *Spitzer*. These power spectra are calculated from the images where $S \geq 50$ mJy sources are removed, and are consistent with the shot (Poisson) noise due to $S < 50$ mJy sources. Moreover, the fluctuation power is consistent with the view of strong evolution in the galaxy counts at 50-200 mJy, which can be interpreted as the emergence of a huge number of Ultra-luminous or Hyper-luminous infrared galaxies at $z \sim 1$ (Pearson 2001, Takeuchi et al. 2001).

Not only the Poisson noise arising from the discrete nature of the galaxies, but also the angular correlation (clustering) of the galaxies are expected to contribute to the power of the surface brightness fluctuations (Peebles 1980). The observed fluctuation power, however, shows no evidence for any contribution from galaxy clustering. Thus, the major scientific goal of the fluctuation studies with AKARI and *Spitzer* is to confirm the existence of the fluctuation power due to clustering, and to estimate the redshift of the galaxies responsible for the clustering. For this purpose one should perhaps examine the cross-correlation of multi-color images in order to isolate the fluctuation power due to sources over some redshift range (say, $z \sim 1$ or $z \sim 2$). The signal-to-noise ratio of the images should be high enough to obtain the fluctuation power due to $z \sim 2$ ULIRGs ($S \sim 10$ mJy). Clearly the AKARI all-sky survey is not adequate since the flux limit is higher than the source confusion limit, and thus the slow-scan mode observation is mandatory (see Table 3, 5). Figure 10 also shows the expected contribution of the detector noise in the slow-scan observation mode. Regarding the required area for the survey, one should also take into account of the field-to-field variation of the clustering signal (*i.e.* cosmic variance). As we have shown in the previous subsection, a survey area of order 10 deg^2 is required to investigate the clustering due to $z \sim 1$ galaxies. The low-frequency noise due to the Galactic infrared cirrus (cirrus noise) should be also minimized and is discussed in subsection 4.2. Moreover, the survey area should be contiguous, in order to confirm the existence of the cirrus noise at a few degrees scale, and to judge whether the cirrus noise will not a problem at higher spatial frequencies.

The survey area and depth requirements to obtain the desired scientific objectives described in this subsection are summarized as follows:

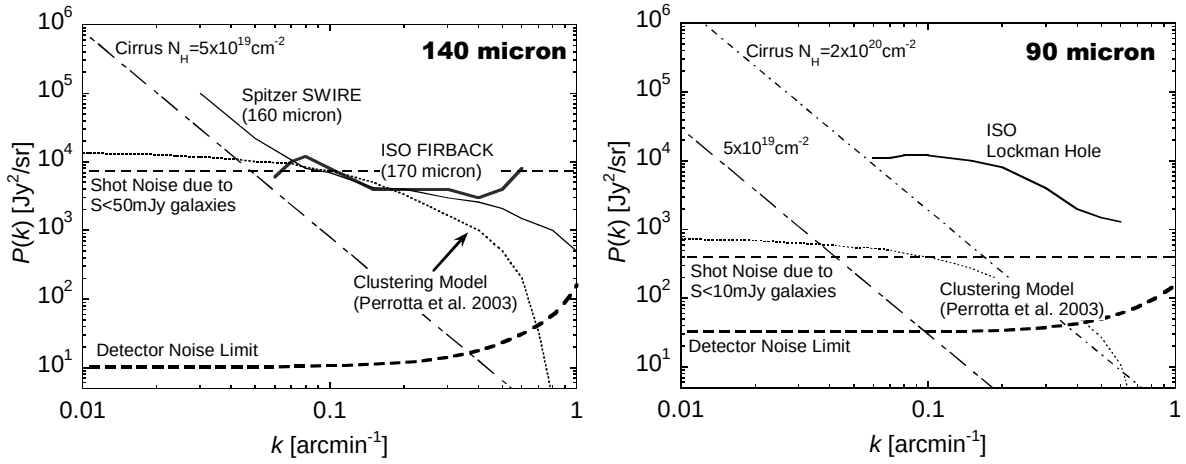

Fig. 10. Angular power spectrum of the CIRB fluctuation in the far-infrared. Results of the ISO/FIRBACK 170μm survey in ELAIS N2 (Puget, Lagache 2001), ISO 90 μm survey in Lockman Hole (Matsuhara et al. 2000): $N_{\rm HI} < 10^{20}$ cm^2, and recent preliminary analysis of Spitzer/SWIRE 160 μm survey (Grossan, Smoot 2005), are also shown. Shot noise (thin dashed lines) is estimated for randomly distributed background galaxies fainter than 10 and 50 mJy at 90 and 160 μm, respectively. The data at 160(170) μm show better agreement with the galaxy clustering model (dotted, Perrotta et al. 2003) than the shot noise case. For comparison, the cirrus power spectra for $N_{\rm HI} = 5 \times 10^{19}$ cm^2 (in the low-cirrus region near SEP) and 2×10^{20} cm^2 are also shown by dash-dotted lines. The AKARI sensitivities (thick dashed lines) calculated by assuming a white noise spectrum correctecd for the spectra of the point-spread function are far below the expected background fluctuation power.

- survey depth: for the study of the cosmic near-infrared background fluctuations, the survey area should be a contiguous, 2-4 degrees wide, circular or square shape. The sensitivity requirement is easily achieved with the exposure time of a single pointing observation. Good stability of the detector array is a key issue to obtain a reliable signal of the background fluctuations at low spatial frequencies.
- survey area: for the study of the cosmic far-infrared background fluctuations, the signal-to-noise ratio of the images should be high enough to obtain the fluctuation power due to $z \sim 2$ ULIRGs ($S \sim 10$ mJy at 90-140 μm), and hence requires the slow-scan observation mode. a survey area of order 10 deg^2 is required to investigate the clustering due to $z \sim 1$ galaxies.

3.4. Statistical study of buried AGN

Not only the cosmic star formation history but also the birth and evolution of Super-Massive Black Holes (SMBHs) are major science goals of modern astronomy. Moreover, the birth and evolution of the SMBHs is closely related to the evolution of the host galaxies, as indicated by the tight correlation between the mass of SMBHs and the velocity dispersion of the bulge component of host galaxies (*e.g.* Meritt & Ferrarese 2001) in the local universe. Furthermore, results from recent hard X-ray surveys have revealed that most of the accretion

onto the SMBHs is obscured by dust (Ueda et al. 2003) prohibiting a diagnostic study by optical lines ("buried AGN"). In such buried AGNs most of the AGN luminosity is absorbed by dust and re-radiated in the mid to far-infrared. Thus in order to unveil the nature of such buried AGN, infrared observations with AKARI will play a key role. Moreover, to discriminate between the hot dust emission powered by AGNs and the warm dust emission powered by star formation, multi-color data at optical to far-infrared wavelengths is particularly useful. This will also enable us to understand the AGN contribution to the CIRB, especially at far-infrared wavelengths.

As described in section 3.2 the proposed NEP survey will provide a huge number of ULIRGs or Hyper-luminous infrared galaxies (HLIRGs) out to $z = 3$, and these samples will provide a unique database to investigate the contribution of the buried AGN as the energy source for the ULIRGs. One should note that such studies will be more effective when observing time is allocated to XMM/Newton hard X-ray imaging of the NEP AKARI deep field.

Another diagnostic tool to investigate the energy sources of ULIRGs are the dust features in the thermal infrared. Since the energy source for the buried AGN is, by definition, concentrated at the center of the dust cloud, its presence is traced by the carbon dust absorption feature at 3.4 μm and the 10-20 μm silicate dust features. So far 6-11 μm spectra of many ULIRGs with ISO (Rigopoulou et al. 1999) and ground-based L-band spectra (Imanishi, Dudley 2000) have been obtained. However, the limited wavelength coverage made it very difficult to determine whether the spectra were dominated by strong 7.7 μm polycyclic aromatic hydrocarbon (PAH) emission features (starburst-powered) or a strong 9.7 μm absorption feature of silicate dust implying the presence of a buried AGN.

The AKARI/IRC incorporates slitless spectroscopic functions at 2-26 μm with a spectral resolving power of 30-90, suitable for the study of relatively broad spectral features. Therefore, we will perform an unbiased spectroscopic survey by using the slitless spectroscopic mode in order to provide numerous SED samples of various galaxy types including the serendipitous detection of buried AGN candidates. Moreover, it is noted that the studies with 3.3 μm PAH feature of local starburst galaxies as well as with the 3.4 μm feature of local AGNs are impossible with *Spitzer*/IRS, due to the lack of wavelength coverage below 5 μm.

The survey area and depth requirements to obtain the desired scientific objective described in this subsection are summarized as follows:

- survey depth and area requirements for the imaging surveys are already stated in the summary of section 3.2. The buried AGN population is an important subset of the entire galaxy sample. Detailed discussion will be given in a separate paper by Pearson et al. (2006).
- survey depth and area requirements for the spectroscopic survey: good sensitivity for the mid-infrared dust features is a key issue in order to generate a sample of unbiased mid-infrared SEDs of galaxies in sufficient numbers . This will be also discussed in a separate

paper.

4. Optimization of the Location of the Survey Fields

In this section, we describe the best location of the survey area for the extragalactic deep survey with AKARI. In short, we first examined the visibility constraint of the AKARI spacecraft which leads us to conclude that the ecliptic pole regions are the almost unique choice, and then checked if the survey will suffer from the confusion noise due to the Galactic infrared cirrus, and also investigated the density of bright sources (mostly stars in the Galaxy) which may cause serious saturation of the near-infrared detectors.

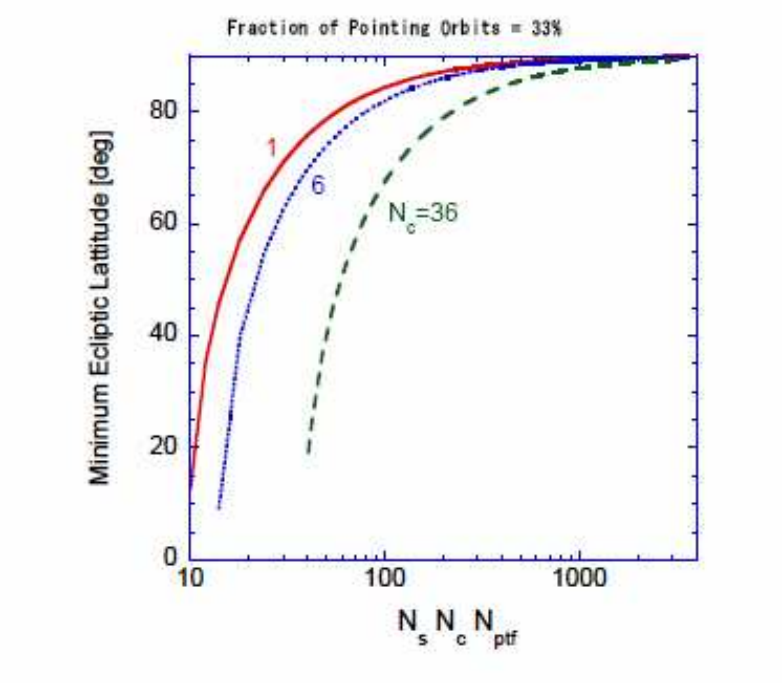

Fig. 11. The minimum value of ecliptic latitude (β) as a function of the number of IRC pointing observations. The figure shows the minimum latitude at which surveys of $N_{\rm c}$=1, 6, 36 number of Field of Views (FOV) in the cross scan direction can be made. The FOV of the IRC is approximately 10×10 arcmin^2, so 6 FOVs in the cross scan direction ($N_{\rm c}$=1, 6) corresponds to 1 degree. The number of pointing observations in the in-scan direction are given by $N_{\rm s}$ and the number per FOV (i.e. the depth) is given by $N_{\rm ptf}$.

4.1. Visibility constraint of AKARI

According to the attitude control scenario described in section 2, we checked the sky visibility constraint for the deep surveys which require a significantly large number of pointed observations. For simplicity we assume a rectangle survey area of uniform depth at an ecliptic latitude β, satisfying the following equation :

$$N_{\rm c} N_{\rm s} N_{\rm ptf} \leq \frac{10 N_{\rm c} + 120}{\Delta\lambda_0 \cos\beta}, \quad (1)$$

where $N_{\rm c}$, $N_{\rm s}$, and $N_{\rm ptf}$ are the number of FOV in the cross-scan direction, number of FOV in the scan direction, and the number of pointed observations per field-of-view respectively. $\Delta\lambda_0 = 4.1$ arcmin is the longitudinal separation between successive orbits at the ecliptic plane. This equation gives the minimum β at which we could perform a survey with a total number of pointed observations $N_{\rm c} N_{\rm s} N_{\rm ptf}$, and is shown in Figure 11.

For example, 1 deg^2 coverage with 30 pointings per FOV requires $N_{\rm c} N_{\rm s} N_{\rm ptf} \sim 1000$. Clearly such a required number of pointing opportunities can only be allowed in the regions very close to ecliptic poles ($\beta \geq 89$ deg) unless the survey area is a long strip or a thin donut. Such geometries do not satisfy the requirement from the scientific objectives described in section 3. Hence the deep survey field must be chosen at the ecliptic polar regions.

4.2. Confusion due to the infrared cirrus emission

An important sensitivity limitation arises due to the spatial fluctuation of the IR cirrus. Helou, Beichman (1990) have assumed that the fluctuation power is proportional to $\bar{B}_\nu^3$ for all wavelengths, where $\bar{B}_\nu$ is mean brightness of the IR cirrus. They have expressed the cirrus confusion noise in the following equation :

$$\frac{\sigma(\lambda)}{1\,{\rm mJy}} = 0.73 \left(\frac{\lambda}{100\,\mu{\rm m}}\right)^{2.5} \left(\frac{D}{0.7{\rm m}}\right)^{-2.5} \left(\frac{\bar{B}_\nu}{1\,{\rm MJysr^{-1}}}\right)^{1.5} \quad . \quad (2)$$

Thus the cirrus confusion noise will depend not only on the variation of the surface brightness of the background structure, but also on the resolution of the telescope (λ/D), resulting in less noise at shorter wavelengths. Kiss et al. (2001) have analyzed 40 sky regions with the ISOPHOT instrument on ISO concluding that the cirrus noise was consistent to within a factor of 2 according to the formulation of Helou, Beichman.

Figure 12 shows the IRAS 100 μm map (Schlegel et al. 1998) near the ecliptic poles. Unfortunately, as shown in the figure, the ecliptic poles are not optimal areas for the local minimum of the infrared cirrus: 2-3 MJy sr^{-1}. Applying equation 2 to the AKARI FIS/IRC wavebands and assuming a range of mean brightness for the infrared cirrus at 100 μm ($\bar{B}_{100}$) with the infrared cirrus SED of Dwek et al. (1997), we obtain the results for the cirrus confusion noise in Table 5. Unless a relatively bright cirrus region ($\bar{B}_{100} \geq 5\,{\rm MJy\,sr^{-1}}$) is observed, the cirrus confusion is not problematic for IRC bands. It is noteworthy that, based on recent *Spitzer* observations at 24 μm in a bright cirrus region in Draco ($N_{\rm HI} = 4 - 14 \times 10^{20}\,{\rm cm^{-2}}$), Dole et al. (2004) reported a rather weak effect leading to a completeness degradation of only 15%.

However, the cirrus noise toward the ecliptic poles is appreciable for the FIS bands (especially LW channels). Hence, we should carefully choose any deep field for FIS imaging, especially for the studies of CIRB fluctuations. One should also take into account any angular frequency dependence of the fluctuation power spectrum of the cirrus : $P(k) \propto k^{-3}$ (Gautier et al. 1992, Kiss et al. 2001, Jeong et al. 2005), where k is the angular frequency. Fluctuations at

large angular scales (order of a degree) are likely to be dominated by cirrus noise, even though the point source detection (*i.e.* at high angular frequency) is not affected. Hence a low-cirrus region is required, especially for the CIRB study in the far-infrared. The optimum area for such far-infrared deep surveys is the low cirrus region in the South or in the ELAIS N1 field ($\bar{B}_{100} \leq 0.5\,\mathrm{MJy\,sr^{-1}}$, corresponding to a hydrogen nuclei column density of 5×10^{19} cm^{-2}) as shown in Figure 12. Figure 10 shows the expected cirrus power spectra toward the low cirrus region near the SEP, compared with the "shot noise" due to the unresolved galaxies. The advantage of the low cirrus region near the SEP can be clearly seen.

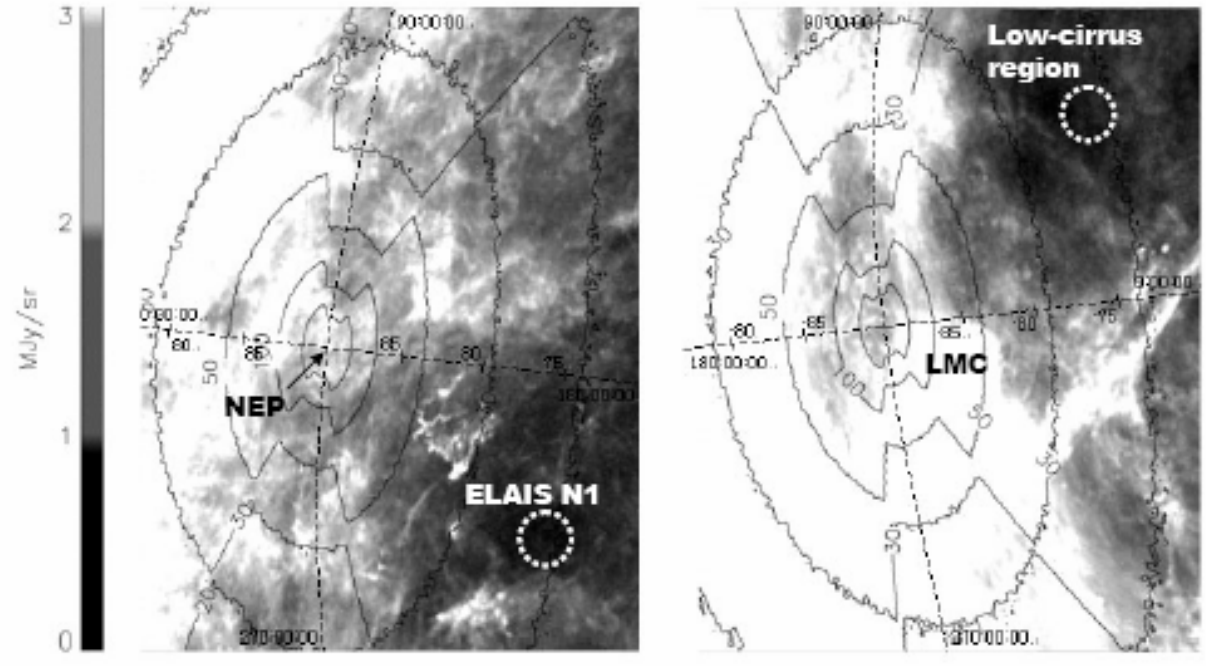

Fig. 12. IRAS 100μm map near the NEP (left) and SEP (right), overlayed on the visibility contours. Darkest areas are approximately 0.3 MJy/sr, and brightest areas correspond to 3 MJy/sr. ELAIS N1(a *Spitzer*/SWIRE field) and the low-cirrus regions from Schlegel et al. (1998) are indicated.

4.3. Bright Stars

Bright stars in our Galaxy as well as the Magellanic clouds should be avoided for extragalactic deep surveys. Not only the saturated pixel due to the bright stars but also the adjacent pixels may not be useful for deep imaging because such pixels are affected by an increased photon noise. $K \leq 12$ mag corresponds to the saturation limit of the N2 band imaging of IRC. However, since the FOV of the IRC is as wide as $10' \times 10'$, it is difficult to find fields without any bright stars in the ecliptic polar regions. In Figure 13 the density distributions of bright 2MASS stars ($K \leq 12$ mag) are shown with the AKARI visibility contours. At the NEP approximately 5 such stars exist per FOV of the IRC. Below $K \simeq 15$ mag extragalactic sources begin to dominate the source counts, and the photon noise due to the stars is not appreciable.

Table 5. Estimated confusion limits in AKARI wavebands. Cirrus noise is calculated assuming the model of Helou & Beichman (1990)

Band	λ_c	Galaxy confusion (5σ μJy)		Cirrus Confusion (5σ μJy) for $\bar{B}_{100}$		
(IRC)	(μm)	40 beam/source	20 beam/source	0.5 MJy/sr	3 MJy/sr	10 MJy/sr
N2	2.43	<1	<1	<1	<1	<1
N3	3.16	<1	<1	<1	<1	<1
N4	4.14	<1	<1	<1	<1	<1
S7	7.3	1	<1	<1	<1	<1
S9W	9.1	3	<1	<1	<1	1.1
S11	10.7	7.9	2	<1	<1	1.6
L15	15.7	50	16	<1	1.1	6.9
L18W	18.3	134	66	<1	1.6	9.5
L24	23.0	257	134	<1	3.1	19.
Band	λ_c	Galaxy confusion (5σ mJy)		Cirrus Confusion (5σ mJy) for $\bar{B}_{100}$		
(FIS)	(μm)			0.5 MJy/sr	3 MJy/sr	10 MJy/sr
N60	65	3.0		0.06	0.91	5.5
WIDE-S	90	7.0		0.33	4.8	29.
WIDE-L	140	45		9.2	135.	823.
N160	160	50		12.	173.	1050.

By using the star count model of the Galaxy (Nakajima et al. 2000), we estimated approximately on average 50 stars per FOV down to $K \sim 15$ mag. When considering the current best estimate for the in-flight point spread function of the IRC-NIR channel (approximately 10 pixels per source in the 70% energy circle), this means approximately only 0.3% of pixels will suffer from saturation or the increased photon noise due to stars. In the case of the SEP, as shown in Figure 13 the surface density of the Galactic stars is about twice larger than that at NEP since it is close to the Large Magellanic Cloud. In conclusion, the surface density of the Galactic stars is non-negligible but still within acceptable limits to perform the extragalactic surveys. Thus for the near and mid infrared deep surveys with AKARI, we select the field near NEP simply because the star density is a factor of two smaller at the NEP, and moreover, we cannot allocate so many pointed observations for extragalactic surveys near SEP because of the existence of another large-area survey with AKARI: the LMC survey.

The bright stars will give serious damages on the optical pre-survey images. Hence the field position was chosen to avoid saturation of the CCDs of the Suprime-cam instrument by bright ($V \leq 10$ mag) stars (see section 7).

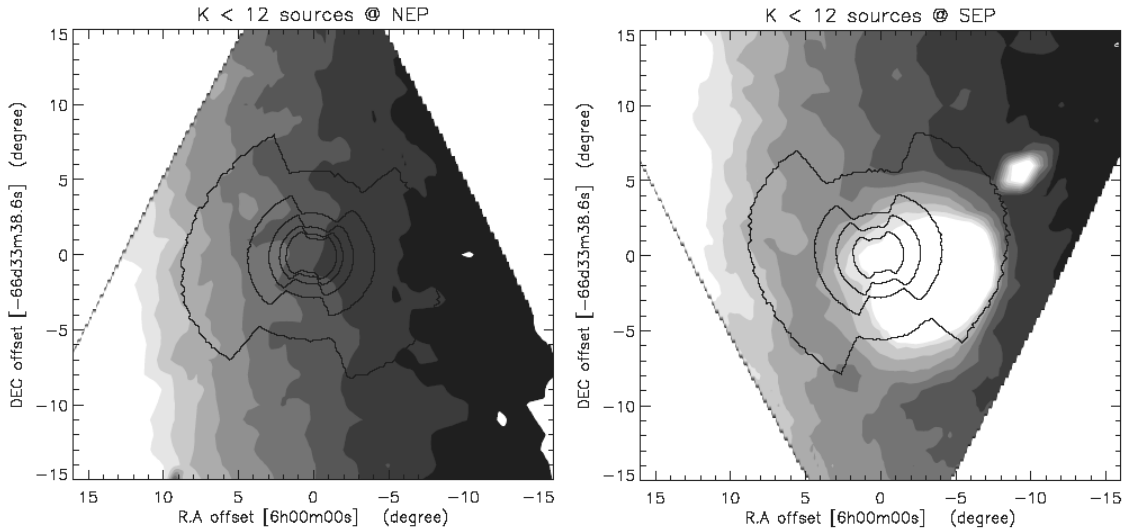

Fig. 13. Bright K<12 2MASS source density around NEP region(left) and SEP region(right). AKARI visibility contours (solid lines) are shown for 250, 200, 150, 100, 50 (in phase 1 plus 2) away from the pole. Gradient corresponds to 130(darkest), 160, 190, 220, 260, 290, 320, 350, 380, 410 stars per square degree.

5. Observation Plan

5.1. Proposed Area for the deep potinting surveys

From the above discussion, regarding the IRC deep survey field, the NEP is the best candidate because approximately 1000 pointing observations can only be realized within a few degrees from NEP (see Figure 11), and there are no other serious limitations. There is an option to move "NEP-Wide" survey field to ELAIS N1 field, one of the *Spitzer*/SWIRE fields. However, the ecliptic latitude of the ELAIS N1 is not high enough to be observable in all the year, and thus it is hard to generate a circular or nearly rectangular map which is one of the key requirements for the study of the cosmic near-infrared background fluctuations (see section 3.3). In contrast, the SEP is not so good for the IRC extragalactic deep survey due to its proximity to the LMC, and moreover, there exists a large-area survey program toward the LMC which makes it difficult to allocate a large number of pointed observations for any extragalactic survey. Thus, for the near and mid infrared deep extragalactic surveys we conclude the NEP is the best target field.

Regarding the far infrared deep surveys, the NEP is acceptable since the cirrus confusion limit is approximately the same or below the galaxy confusion limit considering a mean cirrus brightness (at IRAS 100 μm) of $\bar{B}_{100} = 1 - 2$ MJy/sr and $\bar{B}^3$ dependence of the fluctuation power spectrum (Gautier et al. 1992, see Table 5). However, an extremely-low cirrus region is preferable since the major scientific goal, measurement of the CIRB fluctuations over degree scales, will be hampered by the k^{-3} dependence of the infrared cirrus emission, where k is angular frequency. As shown in Figure 12 alterantive candidate fields are the ELAIS N1 field

near the NEP and the low-cirrus region ner the SEP at $\beta = -74$ deg, where $\bar{B}_{100}$ is as low as 0.2 MJy/sr (Schlegel et al. 1998). The advantage of the ELAIS N1 field near the NEP is that there are numerous multiwavelength data sets already available including the *Spitzer* data. However, pointed observations for the NEP survey (with the IRC) severely conflicts with those for the ELAIS N1 fields, and a large-area survey (more than 10 deg^2) is not realistic. On the other hand, pointing opportunities for the SEP low-cirrus region do not conflict with those for the LMC survey (*i.e.* the locations are different in ecliptic longitude), and thus we conclude that the SEP low-cirrus region is the best target field for the far infrared deep slow-scan surveys. In Table 1 we summarize the overview of the currently planned deep surveys.

5.2. The NEP survey

In this subsection we describe the details of the current observation plan for the NEP survey with AKARI in its pointing attitude mode. In order to satisfy the scientific requirements (section 3), the survey area should be observed to a suitable depth for the detection of statistically meaningful samples of extragalactic sources ($\gg$1000) out to z=4 in the near infrared, and to z=3 in the mid infrared. Moreover, the survey area should be large enough so that the obtained sample does not suffer from serious uncertainty due to cosmic variance, and the geometry of the area should be a circle or a square, *i.e.* a strip or ring should be avoided.

Currently the following two blank-field surveys are planned:

- **NEP-Deep:** deep (28 pointing observations per field-of-view) survey over approximately 0.5 deg^2
- **NEP-Wide:** wide and shallow (2 pointing per FOV) survey of approximately 6.2 deg^2. The survey region is a circular area surrounding the "NEP-Deep" field.

For the former, the one-filter AOT will be used (8-10 pointing observations per filter and per field-of-view) while for the latter, the three-filter AOT will be used. Therefore data will be obtained in all 9 IRC wavebands. The locations of the survey fields is shown in Figure 14. The total number of pointed observations amounts to 954. During phase-1 and the first six months of phase-2, approximately 2.6 pointing opportunities per day using mainly the orbits passing the SAA will be allocated for the survey. Pointing directions are primarily determined by the requirements from the IRC observations: the FIS will be operated in the FTS mode (probably in low spectral resolution mode of approximately 1 cm^{-1}) in parallel, in order to obtain the 50-180 μm SED of the diffuse emission. Although the FTS mode is not sensitive enough to obtain the spectrum of each extragalactic source, these FTS observations toward the NEP are useful for the study of the CIRB as well as Galactic interstellar matter, by using several hundreds of pointing opportunities in this parallel mode.

5.2.1. The Deep survey "NEP-Deep"

The survey area of "NEP-Deep" is a circular area whose center is slightly offset from the NEP, in order to cover the deep pre-survey field which has been already surveyed at optical wavelengths with Subaru/Suprime-cam (see section 7). The survey field is observable for many orbits during the mission, when the offset control is applied. This will be important if we are to cover the field with all IRC channels efficiently. This reasoning is explained as follows: first, as shown in Figure 3 the FOV of the MIR-L channel is offset from those of the NIR and MIR-S channels by approximately 20 arcmin, thus one pointing observation provides a NIR/MIR-S image and a MIR-L image separately on the sky. Secondly, since the FOV configuration rotates 180 deg in approximately 6 months, another pointing observation after 6 months enables us to obtain the corresponding images in the complementary channel. Then two $10' \times 10'$ fields separated by approximately 20 arcmin have been covered with all IRC channels. Therefore, allocation of the same number of pointed observations in both phase-1 and phase-2 (first 6 months) is a mandatory requirement for the "NEP-Deep" survey. Since the 0.5 deg^2 corresponds to 18 independent FOV, 28 pointing per a FOV results in 504 pointed observations in total with just one half of them being executed in Phase-1. Table 6 summarizes the expected flux limits for the NEP survey.

5.2.2. The Shallow-Wide survey "NEP-Wide"

The survey region of "NEP-Wide" is selected to surround the "NEP-Deep" field but is a circular area whose center coincides with the NEP. Unlike the "NEP-Deep" the offset control is not actively used, but the pointing directions are regularly placed (*i.e.* FOVs are primary ordered in the in-scan direction, then the sky coverage is expanded in the cross-scan direction as the scan path rotates) so that the every portion of the survey field is covered with a uniform depth of 2 pointing per FOV in three filter mode (AOT-03). In this manner the survey field will be covered by both the NIR/MIR-S and the MIR-L over a year (phase-1 plus the first six months of phase-2). Currently we plan to allocate 450 pointed observations in total, resulting in 225 independent FOVs corresponding to approximately 6.2 deg^2.

The driving force of the "NEP-Wide" survey is to perform a survey of as large area as possible especially in N2 band of the IRC in the search for the large-scale fluctuations of the cosmic near infrared background (section 3.3). For the mid infrared channels, the main purpose of "NEP-Wide" is to overcome effects due to the cosmic variance at z=0.5-1: as shown in Figure 6 the survey volume of "NEP-Deep" is clearly too small. In addition, it is also noteworthy that more than 1000 ultra or hyper-luminous infrared galaxies ($L_{\rm IR} \geq 10^{12}\,L_{\odot}$) per square degree will be detected by this shallow-wide survey (250μJy at 24μm, Pearson 2005) at $z = 2 - 3$.

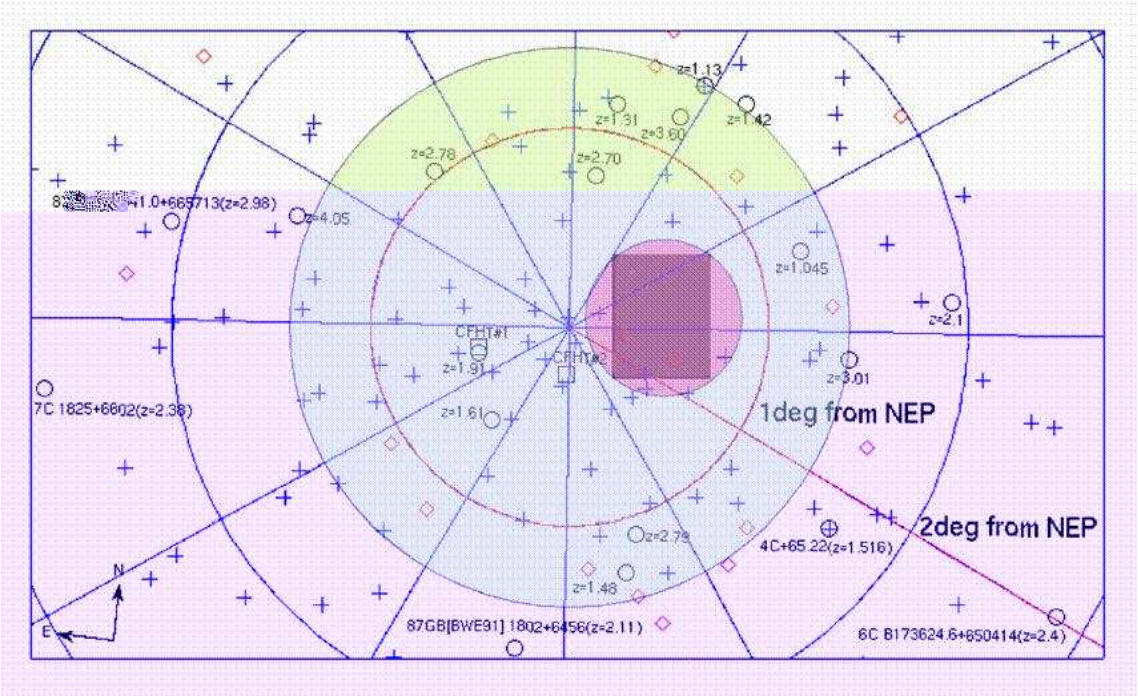

Fig. 14. Survey area planned for the NEP survey in pointing mode, consisting of a circular area ("NEP-Deep", smaller one surrounding the rectangle) with 28 pointing per FOV and a larger circular area ("NEP-Wide", centered at NEP) with 2 pointings per FOV. Also shown are the optical deep survey field with Subaru/suprime-cam (rectangle area) as well as the location of ROSAT X-ray clusters (red diamonds, Gioia et al. 2003), ROSAT galaxies, AGN, planetary nebulae (blue crosses), and high-z radio sources (circles, Brinkmann et al. 1997).

5.2.3. The spectroscopic survey

In addition to the broad-band imaging surveys, slitless spectroscopy in all IRC channels is also planned which will provide another unique product from the AKARI mission : an unbiased near and mid infrared spectroscopic sample of galaxies (see section 6.2). IRS spectroscopic follow-up of relatively bright ($\geq$0.75mJy) 24 μm sources has revealed the nature and the redshift of the sources to some extent (Houck et al. 2005), however, the sample is biased to relatively bright sources. Within a 1 deg radius circle from the NEP, an approximately 2000 arcmin^2 area will be surveyed using the spectroscopic channels (table 4) as part of an AKARI MP. The details will be described in a separate paper.

5.3. Near SEP Survey

Here we describe the details of current observing plan toward the low-cirrus region near the SEP using the FIS slow-scan mode. The target area is shown in Figure 15. Since the major science goal of this survey is to perform a study of the CIRB fluctuations of degree scales or larger, contiguous mapping in an area over at least 15 deg^2 is planned. Considering the

Table 6. IRC flux Limits expected for the NEP survey

Band (IRC)	λ_c (μm)	NEP-Deep[#] (5σ, μJy)	NEP-Wide[$] ($5\sigma$, μJy)
N2	2.43	2.8	12
N3	3.16	1.2	5.5
N4	4.14	2.3	11
S7	7.3	10	49
S9W	9.1	9	39
S11	10.7	12	56
L15	15.7	22	100
L18W	18.3	31	130
L24	23.0	57	270
Band (FIS)	λ_c (μm)	(slow-scan)* (5σ, mJy)	(all-sky survey) † (5σ, mJy)
N60	65	35	100
WIDE-S	90	7	20
WIDE-L	140	4.5	40
N160	160	9	70

[#] AOT-00 (single filter per pointing). Net exposure times : 4000-5000 sec per filter.

[$] AOT-03 (3 filters per pointing). Net exposure times : 200-230 sec per filter.

* assumes four slow-scans with a speed of 15"sec^{-1} at each sky position.

† achieved by integrating the all-sky survey data of all overlapping scans toward the "NEP-Wide" field.

visibility of the low cirrus region at $\beta \simeq 74$ deg, a daily allocation of 3-4 pointing opportunities is mandatory to create such a contiguous map. In Figure 15, an example of the footprints of the FIS FOV are also shown as blue boxes: in this scenario, at each pointing observation, the FIS FOV makes a round trip (240sec forward-scan, then 240sec backward, with 15"/sec scan rate) along the nominal survey path, resulting an $8' \times 1$ deg strip map. Using 270 pointing opportunities over the 90 days when the low-cirrus region is visible (this corresponds to 3 pointing opportunities per day), 3 (along the scan) $\times$ 90 (cross-scan, with 4 arcmin steps) mosaics of the $8' \times 1$ deg strip maps corresponds to an approximately 15 deg^2 fan-shape area.

Figure 16 compares the depths and areal coverage for various slow-scan rates for a fixed number (270) of pointed observations. The expected sensitivities of the WIDE-L and N160 bands reach below the galaxy confusion limit even in case of the fastest scan rate (30"/sec),

and hence the adoption of the faster scan rate is adequate in order to expand the survey area. It is also worth noting that the all-sky sensitivity does not reach the confusion limit even if we take into account the large number of overlapping scans expected near the ecliptic poles.

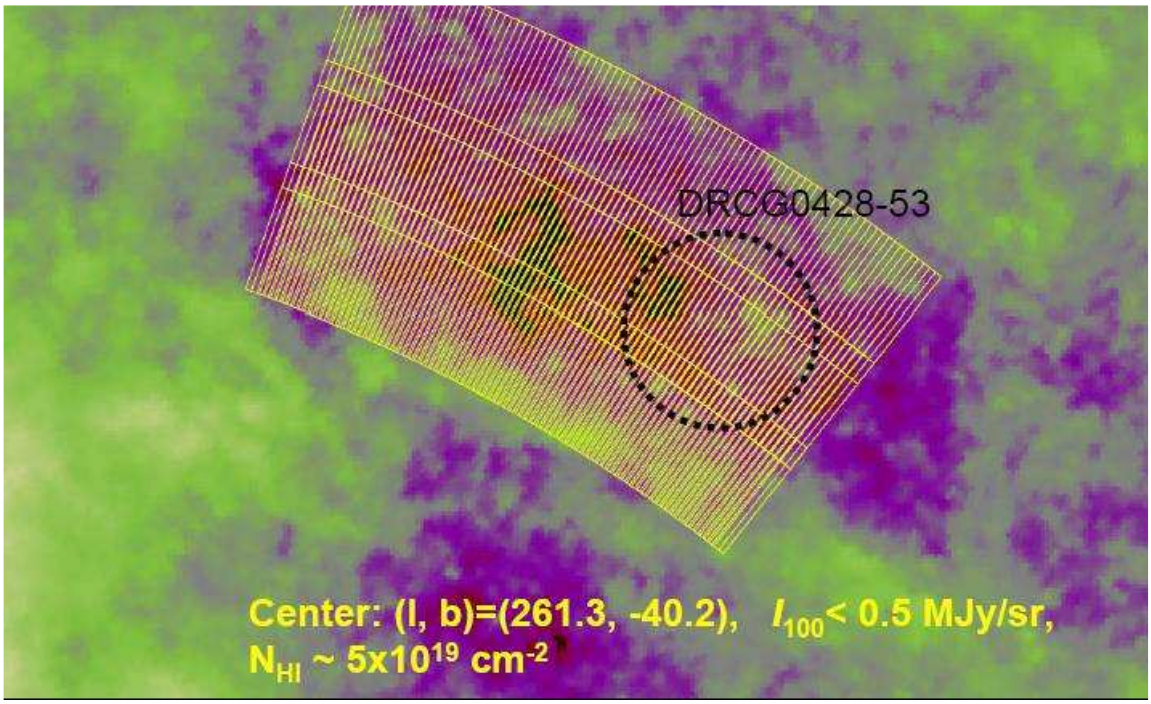

Fig. 15. Areal coverage planned for the low-cirrus area survey near the SEP with FIS slow-scan mode. The fan-shape area (approximately 15 deg^2, blue boxes) will be obtained by mosaicing the strip maps, each of which is obtained in one pointing opportunity.

6. Uniqueness of the Surveys

We discuss the uniqueness of the AKARI deep surveys compared to other contemporary surveys carried out with previous and ongoing missions.

6.1. Infrared Space Observatory

The *Infrared Space Observatory* (ISO, Kessler et al. 1996) launched in November 1995 was equipped with a 60 cm cooled telescope and had the capability for near and mid infrared imaging: *ISOCAM*, a $3' \times 3'$ field of view camera with 32×32 pixels. Most of the deep ISOCAM surveys utilized two broad band filters; LW2 at 6.7 μm and LW3 at 15 μm. In particular, the ISOCAM 15 μm surveys covered a wide range in both sensitivity and spatial area: 0.013 deg^2 with 100 μJy, $0.3 \sim 0.4$ deg^2 with 0.5-0.8 mJy, and 13 deg^2 with 1 mJy (Genzel, Cesarsky 2000 and references therein), resulting in the discovery of a strongly evolving population of galaxies below 1mJy. This evolving population can be interpreted as the presence of luminous, ultra-luminous and hyper-luminous infrared galaxies at $z \sim 1$ (Pearson 2001, Takeuchi et al.

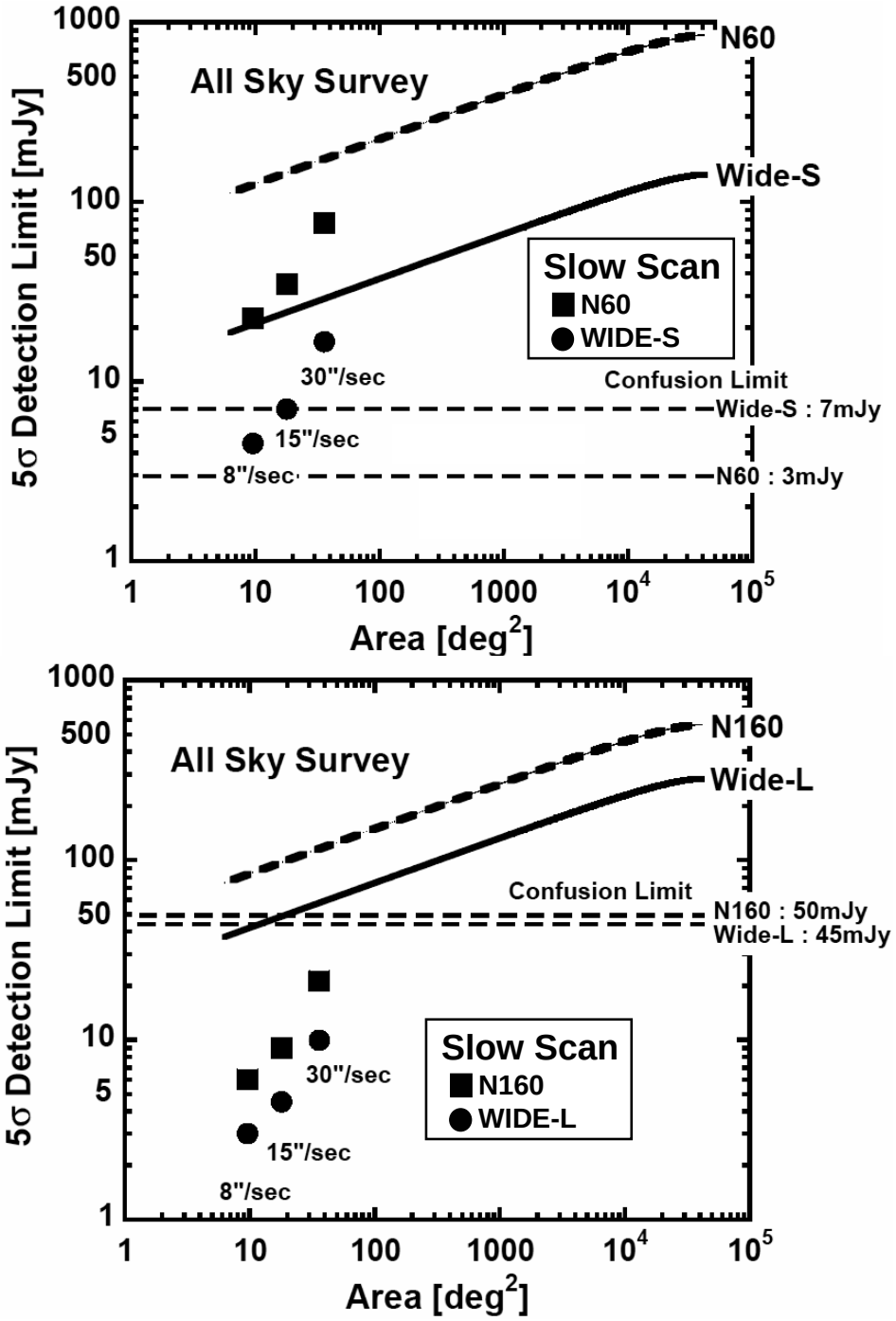

Fig. 16. Depth and areal coverage for various slow-scan surveys with the FIS bands. At each point on this plot, 270 pointing observations are assumed. The resulting areal coverage varies according to the scan-speed: 8, 15, and 30 arcsec/sec. For comparison, the dashed and solid curves show the all-sky survey sensitivities by simply taking into account the number of overlapping scans at any given point on the sky. The horizontal dashed lines are the galaxy confusion limit for a 69 cm telescope estimated based on the recent *Spitzer* results.

2001). These infrared galaxies may be the main contributors to the cosmic infrared background radiation (Takeuchi et al. 2001, Chary, Elbaz 2001). However, the area of the ISOCAM surveys was not large enough to provide sufficient samples of these galaxies when separated into several redshift bins, and the surveys were made solely with the 15 μm band. Hence our knowledge on the star-formation history around $z \sim 1$ is still rather limited.

Thanks to the innovation of the detector technology, the sensitivity in the near and mid infrared of AKARI and *Spitzer* has been improved by an order of magnitude over that of ISOCAM onboard ISO, although the telescope aperture has not increased so much in tandem.

6.2. Spitzer Space Telescope

In August 2003 NASA successfully launched an advanced space infrared observatory, *Spitzer* (Werner et al. 2004). *Spitzer* is an 85cm diameter cooled telescope with three focal plane instruments, IRAC, MIPS, and IRS. The IRAC instrument covers the near to mid infrared wavelengths in 4 bands at 3.6, 4.5, 5.8, 8.0 μm (Fazio et al. 2004), while the MIPS instrument covers the mid to far infrared wavelengths in 3 bands at 24, 70, 160 μm (Rieke et al. 2004). The IRS instrument (Houck et al. 2004) is a low to moderate resolution spectrometer covering 5.2-38 μm with peak-up imagers at 16 and 22 μm (1.2arcmin^2 FOVs).

Spitzer has already completed various wide area surveys, partly for its *Legacy* science projects (SWIRE, GOODS) and partly for the guaranteed time observations. Data products from the first look survey (FLS) and the *Legacy* projects have already been released to the world, and numerous scientific results have already appeared in the literature. Therefore, we should take account the success of *Spitzer* in the design of the AKARI surveys. Besides the major uniqueness as an all-sky surveyor, AKARI also has several unique characteristics in the pointing mode compared to *Spitzer*:

- The 2-26 μm imaging FOV is four times larger in area (approximately $10' \times 10'$) than IRAC,
- Continuous wavelength coverage from 2 to 26 μm, especially in three wavebands (S11, L15, L18W) are available in the 8-24 μm gap of the *Spitzer* bands
- 2.5-5 μm slit spectroscopic capability with moderate resolving power of 140
- 2-26 μm slitless spectroscopic capability with low resolving power of 20-50
- four wavebands at 50-180 μm where *Spitzer*/MIPS has two bands.

Here we describe the uniqueness of imaging capability in more details.

1. FOV of IRC: The large FOV of the IRC compensates for the lower sensitivity per unit observing time. Hence the IRC has similar survey speed to that of *Spitzer*. However AKARI has to carry out the all-sky survey and its mission lifetime is shorter than that of *Spitzer*. Hence, in general *Spitzer* as a mission is superior to make deep as well as wide-area surveys (of order 10's square degrees). Note that the IRC-NIR channel can work even in Phase-3 after Helium boil-off. Thus, for example, with 10 pointing observations per day over a year

in Phase-3, a 50 deg^2 area to the depth of "NEP-Wide" can be surveyed at 2-5 μm.

2. Continuous wavelength coverage from 2-24 μm: the IRC wavelength coverage over the 8-24 μm gap of the *Spitzer* bands (see Figure 2) is extremely useful to estimate the redshift and to unveil the nature of $z = 1 - 3$ galaxies: star-forming galaxies are characterized by the PAH features at rest-frame 3.3, 6.2, 7.7 μm and silicate absorption at 10 μm ("Silicate-break", see Takagi, Pearson 2005), while AGN with dusty torii are characterized by a rather featureless hot dust continuum, occasionally with absorption features of silicate or carbon dust grains. SED fitting to the sources will break any degeneracy in the starburst-AGN phenomenon. Moreover, 11-18 μm surveys which are much deeper and wider than those with ISO are one of the most unique capabilities of AKARI. Although *Spitzer*/IRS has a 16 μm peak-up camera, it covers only 1.2 arcmin^2 FOV. Hence, the IRC can perform surveys with 100 times faster mapping speed.

3. Four wavebands at 50-180 μm: in the far infrared *Spitzer*/MIPS has 70 μm and 160 μm bands, while AKARI/FIS has 4 wavebands. Such multi-color information provided by AKARI/FIS is useful to solve the redshift - temperature degeneracy in interpreting the far infrared SED, since the peak of the dust emission resides in the far-infrared. This is also true for the studies of the CIRB fluctuations : by cross-correlating the faint detected sources or fluctuation images at shorter wavelengths (WIDE-S and N60) and the fluctuation images at longer wavelengths (WIDE-L and N160), we can investigate the typical redshift of the sources contributing the CIRB fluctuations.

By utilizing these unique capabilities, ecliptic pole surveys with AKARI will reveal the dusty star-formation history of the universe, break the degeneracy in the starburst-AGN phenomenon, and unveil the origin of CIRB. Regarding the mid-infrared deep survey with AKARI, one might ask why we do not plan to observe the *Spitzer*/Legacy or FLS fields with solely S11, L15, and L18W. The answer is quite simple: for deep surveys in the pointing mode, except for regions toward ecliptic poles we cannot provide a sufficient number of pointing opportunities to achieve the depth required for the detection of $z = 2 - 3$ objects, as described in section 4.

It is however, worthwhile to consider collaborative surveys with *Spitzer* toward the NEP as well as the SEP low-cirrus regions. For the former, if IRAC 4 band and MIPS 24 μm imaging were carried out, the AKARI/IRC could then concentrate on imaging with 10-20 μm bands and the slitless spectroscopy. In case of the latter survey, besides the FIS slow-scan surveys we cannot undertake $\sim$10 deg^2 IRC surveys because of the relatively low visibility of the field. Thus, IRAC and MIPS shallow, but wide-area imaging will greatly increase the scientific value of the SEP low-cirrus region survey.

7. Coordinated multi-wavelength pre-surveys

To perform our scientific goals, multi-wavelength data in the AKARI deep survey fields at both ecliptic poles are essential in many respects. First of all, the higher spatial resolution of ground-based large telescopes enables us to obtain accurate source positions which are vital for follow-up with optical/near-infrared spectroscopy. Second, high spatial resolution near infrared images can give us the opportunity to classify the galaxy type based on the optical (in rest frame) morphology of the source. Third, multi-colour optical/near-infrared photometric data are useful to estimate the photometric redshift of the counterparts of the AKARI sources by identifying the Lyman-break (LBGs, Steidel et al. 1996, Ouchi et al. 2004), or the 0.4 μm break in their SEDs (such as EROs, Pozzetti, Mannucci 2000, Mannucci et al. 2002, Caputi et al. 2004, Fontana et al. 2004). These techniques are very useful to check and confirm the photometric redshifts estimated from the SEDs using the AKARI wavebands, by using the 1.6 μm bump as well as the silicate/PAH features. We have already obtained preparatory images at the optical/near-infrared bands toward the AKARI survey fields, and here we briefly introduce the current status for future reference.

7.1. NEP pre-surveys

In June 2003, we observed the "NEP-Deep" region with the Subaru/Suprime-cam, where the 3σ limiting magnitudes(AB) reach down to B=28.4, V=27, R=27.4, i'=27, and z'=26.2 over 918 arcmin^2, This has been followed by a successive observation in July 2004 with V and a narrow band filter (NB711). Further near-infrared (J and $K_{\rm s}$) images have been taken with KPNO-2m/FLAMINGOS to a limiting magnitude (Vega) of $K_{\rm s} \sim 20$ mag also in June 2004. Together with the near infrared images, we can identify candidate active star-forming galaxies at $z > 1.4$ by using the BzK technique (Daddi et al. 2004). Comparison of these BzK samples with ULIRGs found by the proposed AKARI deep survey will provide a unique database for the study of the star formation history of the Universe. Furthermore, a larger area of approximately 2 deg^2 has been observed with CFHT/Megacam at optical ($g'r'i'z'$) wavelengths to a 5σ limiting magnitude(AB) of 26 mag in the $g'r'i'$ bands and 24 mag in the z' band. This survey covers a part of the "NEP-Wide" area and will also be useful in identifying candidates for clusters of galaxies. We also plan to obtain a deep U-band images to search for the Lyman-break population at $z \leq 3$.

7.2. SEP pre-surveys

To identify the far infrared sources detected in the FIS slow-scan survey toward the SEP low-cirrus region, optical observations are underway. In 2004 we obtained R-band images over about half of the FIS survey field area to R=25 mag by using the ESO 2m and the CTIO 4m telescopes. Surveys at other wavebands are also under consideration.

7.3. Surveys at other wavelengths

Deep radio images are very useful to identify luminous starburst galaxies. At the NEP, there is an existing 20 cm VLA observation by Kollgaard et al. (1994) to a limiting flux density of 200 μJy over 29.3 deg^2. However, this survey seems to be too shallow to identify the mid infrared sources expected from the deep surveys with AKARI/IRC. For the area centered at the NEP we have already take 21 cm radio images to a limiting flux of 50 μJy by using the WSRT in the Netherlands. A deeper VLA proposal is under consideration.

Submillimeter data are mandatory for the study of the star formation history of the Universe hidden by the dust, since the submillimeter flux (far-infrared in rest frame) is a direct measure of the infrared bolometric luminosity originating from the dust warmed by the stellar light. The SCUBA camera on the JCMT is no longer available for guest observers and thus allocation of the telescope time of the JCMT to the NEP field is very difficult until the commission of the SCUBA-2 camera. The Balloon-borne Large Area Submillimeter Telescope (BLAST)[4] is a promising candidate to obtain submillimeter data for the NEP field. BLAST is a 2-m aperture balloon-borne telescope incorporating 250, 350, and 500 μm imagers with $6.5' \times 13'$ FOV (PI : Dr. Mark Devlin, Univ. of Pennsylvania). Long duration ($\sim$10 days) flights at the South Pole and Alaska have been comissioned from 2005 summer, which will allow 1 deg^2 deep surveys to be made. We are planning a coordinated multi-band survey toward NEP with AKARI and BLAST. With this coordinated survey, we will obtain optical identifications of BLAST sources with multi-band data in a similar manner to that of the SCUBA galaxies with *Spitzer*/MIPS 24 μm fluxes (Egami et al. 2004, Ivison et al. 2004).

UV and X-ray data are also very important. One of the most promising methods for the selection of $1.5 < z < 2.5$ galaxies is the Lyman break technique which requires near UV observations. Moreover, FUV fluxes at $\sim$1500 A are one of the key diagnostics for star formation while the infrared data from AKARI tell us the amount of starlight extincted by the dust. We should seek deep pointing observations with the Galaxy Evolution Explorer (GALEX)[5], which was launched in April 2003. X-ray data are also important in two respects: the X-ray emission from the hot intergalactic medium is useful to search for cluster candidates, and deep X-ray images are necessary to identify buried AGN which may be strong mid-infrared emitters in the AKARI deep images. The ROSAT source catalogues have already been released (Henry et al. 2001, Gioia et al. 2003), and hard X-ray imaging with XMM-Newton is under consideration.

8. Summary

The AKARI observational strategy and the details of the observational plans for the coordinated deep pointing surveys toward the ecliptic poles are described. We have reviewed

[4] see http://chile1.physics.upenn.edu/blastpublic/index.shtml

[5] see http://www.srl.caltech.edu/galex

the scientific goals and requirements for the surveys, as well as the technical constraints of the AKARI spacecraft and effects of the foreground astronomical sources. We conclude that the NEP is the best location for the AKARI extragalactic 2-26 μm deep survey, while the low-cirrus regions near SEP is optimum for the 50-180 μm slow-scan surveys. The ELAIS-N1 field, one of the *Spitzer*/SWIRE fields, cannot be selected as a wide, shallow survey field since its ecliptic latitude is not high enough to generate a circular or nearly rectangular map.

The technical details of the blank-field surveys are as follows:

- "NEP-Deep" 2-26 μm survey: deep (28 pointing observations per field-of-view) survey of approximately 0.5 deg^2 with three filters per each IRC channel, resulting in 504 pointing observations in total(a half is in Phase-1), and
- "NEP-Wide" 2-26 μm survey: wide but shallow (2 pointing per FOV) survey of approximately 6.2 deg^2 with three filters per each IRC channel. The survey region is a circular area surrounding the " NEP-Deep" field, and in total 450 pointing observations are required.
- SEP low-cirrus region survey at 50-180 μm : 15-20 deg^2 fan-shape area survey toward the very low cirrus ($\bar{B}_{100}$ is as low as 0.2MJy/sr) region by using the FIS slow-scan mode with a redundancy of at least two. In total 270 pointing observations are required.

In the same target field of the above imaging surveys, we are also investigating the technical feasibility of IRC's unique slitless spectroscopic capability, in order to construct an unbiased sample of near to far infrared SED templates for various kinds of galaxies at $z < 1$. This will be further described in a separate paper (Ohyama et al. in prep.). Multiwavelength ground-based surveys are also ongoing, and optical images and catalogs will be published soon (Wada et al. in prep.).

Acknowledgements

We would like to thank all AKARI team members for their support on this project. We also thank Dr. David Hughes for discussion on possible collaboration between BLAST and AKARI, Dr. Takamitsu Miyaji for his effort on the X-ray observation plan, and Dr. Patrick Henry for information on the ROSAT clusters toward NEP. This work partly supported by the JSPS grants (grant number 15204013, and 16204013). CPP acknowledges support from JSPS while in Japan.

References

Benítez, N. 2000, ApJ, 536, 571
Bolzonella, M., Miralles, J. -M., Pelló, R. 2000, A&A, 363, 476
Brinkmann, W., Yuan, W., Siebert, J. 1997, A&A, 319, 413
Caputi, K.I., Dunlop, J.S., McLure, R.J., Roche, N.D. 2004, MNRAS, 353, 30
Caputi, K.I., Dunlop,J.S., McLure, R.J., Roche, N.D. 2005, MNRAS, 361, 607

Chapman, S.C., Blain, A.W., Ivison, R.J., Smail, I.R. 2003, Nature, 422, 695
Chapman, S.C., Blain, A.W., Smail, I., Ivison, R.J. 2005, ApJ, 622, 772
Chary, R., Elbaz, D. 2001, ApJ, 556, 562
Collister, A.A., Lahav, O. 2004, PASP, 116, 345
Daddi, E., Cimatti, A., Renzini, A., Fontana, A., Mignoli, M., Pozzetti, L., Tozzi, P., Zamorani, G. 2004, ApJ, 617, 746 (astro-ph/0409041)
Dickinson, M., Papovich, C., Ferguson, H., Bundavári 2003, ApJ, 587, 25
Dole, H. et al. 2004, ApJS, 154, 93
Dwek, E. et al. 1997, ApJ, 475, 565
Egami E. et al. 2004, ApJS, 154, 130
Elbaz, D., et al. 1999, A&A, 351, L37
Fazio, G.G., et al. 2004, ApJS, 154, 10
Fontana, A., et al. 2004, A&A, 424, 23
Franceschini, A., et al. 2003, A&A, 403, 501
Gadner, J.P. et al. 2000 AJ, 119, 486
Gautier, T.N., Boulanger, F., Pérault, M., Puget, J.-L., Guilaine, G., Hivon, E. 1992, AJ, 103, 1313
Genzel, R., Cesarsky, C. J. 2000, ARA&A, 38, 761
Giavalisco, M., et al. 2004, ApJL, 600, L93
Gioia, I.M., Henry, J.P., Mullis, C.R., Böhringer, H., Briel, U.G., Voges, W., & Huchra, J.P. 2003, ApJS, 149, 29
Grossan, B., Smoot, G.F. 2005, preprint(astro-ph/0504167)
Hauser, M.G., Dwek, E. 2001, ARA&A, 39, 249
Helou, G., Beichman, C.A. 1990, in From Ground-Based to Space-Borne Sub-mm Astronomy, proc. of the 29th Liége International Astrophysical Coll., ESA publ., p.117
Henry, J.P., Gioia, I.M., Mullis, C.R., Voges, W., Briei, U.G., Böhringer, H., Huchra, J.P. 2001, apjl, 553, L109
Houck, J. et al. 2004, ApJS, 154, 18
Houck, J. et al. 2005, ApJL, 622, L105
Imanishi, M. & Dudley, C.C. 2000, ApJ, 545, 701
Ivison, R.J. et al. 2004, ApJS, 154, 124
Jeong, W.-S. et al. 2003, PASJ, 55, 717
Jeong, W.-S. et al. 2004, Advances in Space Research, 34, 578
Jeong, W.-S., Lee, H. M., Pak, S., Nakagawa, T., Kwon, S. M., Pearson, C. P., White, G. 2005, MNRAS, 357, 535
Kashlinsky, A. 2005, Phys. Rep., in press (astro-ph/0412235)
Kawada, M. et al. 2004, Proc. SPIE, 5487, 359
Kessler, M.F., et al. 1996, A&A, 315, L27
Kiss, Cs., Ábrahám, P,, Klaas, U., Juvela, M., Lemke, D. 2001, A&A, 379, 1161
Kodama, T., Arimoto, N. 1997, A&A, 320, 41
Kollgaard, R.I., Brinkmann, W., Chester, M.M., Feigelson, E.D., Hertz, P., Reich, P., & Wielebinski, R. 1994, ApJS, 93, 145

Lagache, G. Puget, J.-L., Gispert, R. 1999, Ap&SS, 269, 263
Lagache, G., Puget, J.-L. 2000, A&A, 355, 17
Lonsdale, C. et al. 2004, ApJS, 154, 54
Madau, P., Ferguson, H.C., Dickinson, M., Giavalisco, M., Steidel, C., Gruchter, A. 1996, MNRAS, 283, 1388
Mannucci, F., et al. 2002 MNRAS, 329, L57
Matsuhara, H. et al. 2000, A&A, 361, 407
Matsuhara, H., Shibai,H., Onaka, T., & Usui, F. 2005, Advances in Space Research, 36, 1091
Matsumoto, T. et al. 2005, ApJ, 626, 31
Merritt, D., Ferrarese, L. 2001, ApJ, 547, 140
Murakami, H. 2004, Proc. SPIE, 5487, 330
Nakajima, T. et al. 2000, AJ, 120, 2488
Neugebauer, G. et al. 1984, ApJL, 278, L1
Onaka, T. et al. 2004, Proc. SPIE, 5487, 338
Ouchi, M., et al. 2004, ApJ, 611, 660
Ouchi, M., et al. 2005, ApJ, 620, L1
Oyabu, S., et al. 2005, AJ, 130, 2019
Patris, J., Dennefeld, M., Lagache, G., Dole, H. 2003, A&A, 412, 349
Peacock, J.A., Dodds, S.J. 1994, MNRAS, 267, 1020
Pearson, C. P., Matsuhara, H., Onaka, T., Watarai, H., Matsumoto, T. 2001, MNRAS, 324, 999
Pearson, C.P. 2001, MNRAS, 325, 1511
Pearson, C.P. 2005, MNRAS, 358, 1417
Peebles, P.J.E. 1980, The Large-Scale Structure of the Universe. Princeton Univ. Press, Princeton, NJ
Perrotta, F., Magliocchetti, M., Baccigalupi, C., Bartelmann, M., De Zotti, G., Granato, G. L., Silva, L., Danese, L. 2003, MNRAS, 338, 623
Pilbratt, G.T. 2003, Proc. SPIE, 4850, 586
Pozzetti, L., & Mannucci, F. 2000 MNRAS, 317, L17
Pozzi, F., et al. 2004, ApJ, 609, 122
Puget, J.L., & Lagache, G. 2001, IAU Symposium, Vol. 204, 233
Rieke, G.H., et al. 2004, ApJS, 154, 25
Rigopoulou, D., Spoon, H.W.W., Genzel, R., Lutz, D., Moorwood, A.F.M., Tran, Q.D. 1999, AJ, 118, 2625
Rix, H.-W., et al. 2004, ApJS, 152, 163
Sawicki, M. 2002, AJ, 124, 3050
Schlegel, D.J., Finkbeiner, D.P., Davis, M. 1998, ApJ, 500, 525
Shimasaku, K., et al. 2004, ApJ, 605, L93
Somerville, R.S., Lee, K., Ferguson, H.C., Gardner, P., Moustakas, L.A., Giavalisco, M. 2004, ApJL, 600, L171
Steidel, C., Giavalisco, M., Pettini, M., Dickenson, M., Adelberger, K.L. 1996, ApJL, 462, L17
Takagi, T. & Pearson, C.P. 2005, MNRAS, 357, 165

Takeuchi, T. T., Ishii, T. T., Hirashita, H., Yoshikawa, K., Matsuhara, H., Kawara, K., & Okuda, H. 2001, PASJ, 53, 37
Taniguchi, Y. 2003, J. Korean Astron. Soc. 36, 1 (astro-ph/0306409)
Totani, T., Yoshii, Y., Iwamuro, F., Maihara, T., Motohara, K. 2001, ApJL, 550, L137
Ueda, Y., Akiyama, M., Ohta, K., Miyaji, T. 2003, ApJ, 598, 886
Werner, M.W., et al. 2004, ApJS, 154, 1
Williams, R.E. et al. 1996 AJ, 112, 1335
Williams, R.E. et al. 2000 AJ, 120, 2735
Wright, E.L. 2004, New Astronomy Reviews, 48, 465